

Independent Verification and Validation for Analytical Graphics, Inc. of Three Astrodynamic Functions of the Satellite Tool Kit: Version 4.1.0

15 February 2000

Prepared by

C. C. (George) Chao
Systems Engineering Division

Jesse W. Cook
Systems Engineering Division

John Cox
Systems Engineering Division

Thomas F. Starchville
Reconnaissance Systems
Division

Roger C. Thompson
Reconnaissance Systems Division

Lori F. Warner
Systems Engineering Division

Prepared for

ANALYTICAL GRAPHICS, INC.
Malvern, Pennsylvania

Engineering and Technology Group

INDEPENDENT VERIFICATION AND VALIDATION FOR
ANALYTICAL GRAPHICS, INC. OF THREE ASTRODYNAMIC FUNCTIONS
OF THE SATELLITE TOOL KIT: VERSION 4.1.0

15 February 2000

Prepared by

C. C. (GEORGE) CHAO, JESSE W. COOK, JOHN COX, THOMAS F. STARCHVILLE
ROGER C. THOMPSON, and LORI F. WARNER

Engineering and Technology Group
THE AEROSPACE CORPORATION
El Segundo, CA 90245-4691

Prepared for

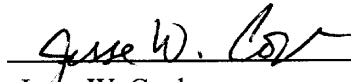
ANALYTICAL GRAPHICS, INC.
Malvern, PA 19355

INDEPENDENT VERIFICATION AND VALIDATION FOR ANALYTICAL
GRAPHICS, INC. OF THREE ASTRODYNAMIC FUNCTIONS OF THE
SATELLITE TOOL KIT: VERSION 4.1.0

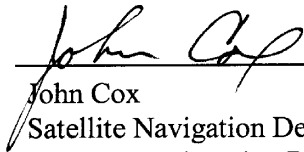
Prepared by



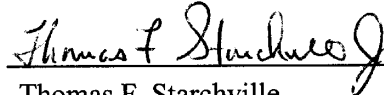
C.C. (George) Chao
Astrodynamics Department
Systems Engineering Division
Engineering and Technology Group



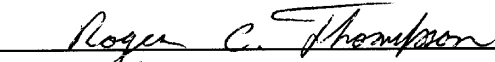
Jesse W. Cook
Satellite Navigation Department
Systems Engineering Division
Engineering and Technology Group



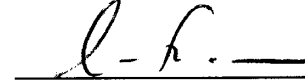
John Cox
Satellite Navigation Department
Systems Engineering Division
Engineering and Technology Group



Thomas F. Starchville
Performance Modeling and Analysis
Reconnaissance Systems Division
Engineering and Technology Group

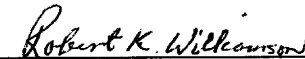


Roger C. Thompson
Performance Modeling and Analysis
Reconnaissance Systems Division
Engineering and Technology Group



Lori F. Warner
Satellite Navigation Department
Systems Engineering Division
Engineering and Technology Group

Approved by



Robert K. Williamson, Principal Director
System Analysis and Simulation Subdivision
Engineering and Technology Group



William H. Hiatt, General Manager
Reconnaissance Systems Division
Engineering and Technology Group

CONTENTS

EXECUTIVE SUMMARY.....	VI
HPOP	VI
PARAMETER AND COORDINATE FRAME TRANSFORMATIONS	VII
ACCESS AND VISIBILITY CALCULATIONS.....	VII
1. HIGH PRECISION ORBIT PROPAGATOR	1
1.1 ASSUMPTIONS AND APPROACH	1
1.2 RESULTS	3
1.2.1 TRACE Closure Tests.....	3
1.2.2 Initial Tests.....	3
1.2.3 Comprehensive Tests.....	8
1.3 CONCLUSIONS	8
2. PARAMETER AND COORDINATE FRAME TRANSFORMATIONS.....	11
2.1 METHODOLOGY	11
2.2 TOOLS AND DATABASES	12
2.2.1 Databases.....	12
2.2.2 Scripts.....	12
2.2.3 Geo.....	12
2.2.4 Rotate.....	12
2.2.5 TRACE	12
2.2.6 Physical Constants.....	13
2.3 VALIDATION PROCEDURES	14
2.3.1 Reference Frames.....	14
2.3.2 Orbit Parameter Sets.....	15
2.3.3 Earth-Fixed Transformations.....	15
2.3.4 Earth Orientation Parameters	15
2.3.5 Validation Environment	15
2.3.6 Validation Limitations.....	15
2.4 VALIDATION RESULTS	16
2.4.1 Validation Case 1 – LEO Orbit.....	16
2.4.2 Validation Case 2 – GPS Orbit.....	17
2.4.3 Validation Case 3 – HEO Orbit.....	17
2.4.4 Validation Case 4 – MEO Orbit.....	18
2.4.5 Validation Case 5 – GEO Orbit.....	18
2.4.6 Validation Case 6 – SEO Orbit.....	19
2.5 SUMMARY	27
3. VALIDATION OF STK ACCESS AND VISIBILITY FUNCTIONS.....	29
3.1 VALIDATION APPROACH	29
3.2 TOOL DESCRIPTIONS AND COMPARISONS.....	29
3.3 SCENARIO DESIGN.....	30
3.3.1 Orbits.....	30
3.3.2 Sensors	30
3.3.3 Targets.....	34
3.3.4 Individual Satellite Visibility Case Naming Convention	34
3.3.5 Satellite-to-Satellite Visibility Case Naming Convention.....	35
3.4 RESULTS	37
3.4.1 Points and Areas	37
3.4.2 Satellite-to-Satellite.....	38

3.5 DATA VERIFICATION TESTS	38
3.5.1 <i>Resolution of the Differences</i>	38
3.6 CONCLUSIONS	40
APPENDIX: ACCESS RESULTS RAW DATA FOR ALL CASES.....	41

FIGURES

FIGURE 1. NADIR – HORIZON SENSOR	31
FIGURE 2. IN-TRACK – HORIZON SENSOR	31
FIGURE 3. CROSS-TRACK – HORIZON SENSOR	32
FIGURE 4. FORWARD-LOOKING SENSOR	32
FIGURE 5. PUSH-BROOM SENSOR	33
FIGURE 6. SIDE-LOOKING SENSOR	33
FIGURE 7. POINT AND AREA TARGET LOCATIONS.....	34
FIGURE 8. GROUND STATION AND POINT TARGET LOCATIONS	36
FIGURE 9. FORWARD-LOOKING SENSOR ACCESS TO AREA TARGET	39

TABLES

TABLE 1. TEST ORBIT INITIAL STATES	2
TABLE 2. TEST CASE ORBIT PARAMETERS	2
TABLE 3. FORCE MODELS APPLIED TO ORBIT TYPES.....	3
TABLE 4. QUALITATIVE SUMMARY OF INITIAL TEST RESULTS.....	4
TABLE 5. TRACE v2.4.9 - STK v4.1.0 ECF POSITION DIFFERENCES	4
TABLE 6. SPHERICAL GRAVITY MODEL TESTS - MAXIMUM TRACE v2.4.9 – STK v4.1.0 DIFFERENCES	5
TABLE 7. WGS-84 EGM96 GRAVITY MODEL TESTS - MAXIMUM TRACE v2.4.9 – STK v4.1.0 DIFFERENCES.....	6
TABLE 8. CELESTIAL PERTURBATIONS TESTS - MAXIMUM TRACE v2.4.9 – STK v4.1.0 DIFFERENCES.....	6
TABLE 9. SOLAR RADIATION PRESSURE MODEL TESTS - MAXIMUM TRACE v2.4.9 – STK v4.1.0 DIFFERENCES.....	7
TABLE 10. ATMOSPHERIC DENSITY MODEL TESTS - MAXIMUM TRACE v2.4.9 – STK v4.1.0 DIFFERENCES	7
TABLE 11. COMPREHENSIVE TESTS - MAXIMUM TRACE v2.4.9 – STK v4.1.0 DIFFERENCES.....	8
TABLE 12. VALIDATION OUTPUT MATRIX	11
TABLE 13. PHYSICAL CONSTANTS	13
TABLE 14. VALIDATION INPUT MATRIX.....	14
TABLE 15. ORBITAL ELEMENTS (METERS, DEGREES)	14
TABLE 16. CASE v1	20
TABLE 17. CASE v2	21
TABLE 18. CASE v3	22
TABLE 19. CASE v4	23
TABLE 20. CASE v5	25
TABLE 21. CASE v6	26
TABLE 22. KEPLERIAN ORBITAL ELEMENTS FOR SCENARIOS	30
TABLE 23. ELEMENTS OF THE SATELLITE-TO-SATELLITE CASES.....	35
TABLE 24. POINT TARGET RELATIVE DIFFERENCES FOR SELECTED CASES	37
TABLE 25. AREA TARGET RELATIVE DIFFERENCES FOR SELECTED CASES	38
TABLE A.1. STK v4.1.0 AND AEROSPACE TOOLS ACCESS RESULTS FOR LEO CASES	42
TABLE A.1 (CONT.). STK v4.1.0 AND AEROSPACE TOOLS ACCESS RESULTS FOR LEO CASES.....	43
TABLE A.1 (CONT.). STK v4.1.0 AND AEROSPACE TOOLS ACCESS RESULTS FOR LEO CASES.....	44
TABLE A.2. STK v4.1.0 AND AEROSPACE TOOLS ACCESS RESULTS FOR HEO CASES.....	45
TABLE A.3. STK v4.1.0 AND AEROSPACE TOOLS ACCESS RESULTS FOR GEO CASES.....	46
TABLE A.4. STK v4.1.0 AND AEROSPACE TOOLS ACCESS RESULTS FOR SATELLITE-TO-SATELLITE CASES	47

Executive Summary

This technical report documents the results of an Independent Verification and Validation (IV&V) of specified functions of the Satellite Tool Kit (STK) of Analytical Graphics, Inc. (AGI). This first phase of the IV&V of STK is focused on three astrodynamics functions: (1) the high precision orbit propagator (HPOP), (2) parameter and coordinate frame transformations, and (3) access and visibility calculations. The Aerospace Corporation's trajectory analysis and orbit determination program TRACE v2.4.9 was used as the benchmark tool for conducting tests for functions (1) and (2). Other Aerospace Corporation programs—Rotate v1.0, Geo v1.0, SOAP v9.2.2 and ASTROLIB (1999 Version)—were used for testing the STK coordinate frame transformations, access and visibility calculations. All of the IV&V testing was made against the released version of 4.1.0 of STK.

The agreements between STK-generated satellite ephemeris or orbit parameters and those generated by Aerospace Corporation programs varied with individual task conditions. A single quantitative statement cannot be made for all testing. Based on Aerospace experience, results ranged from satisfactory to excellent. Some limited areas had larger than expected differences, but differences were deemed small for most applications, with the exception of those involving precision geodesy or altimetry work. The quality of the three STK functions is reflected by the test results of the IV&V documented in this report. It is up to the users to determine the adequacy of STK v4.1.0 for their specific applications.

Detailed descriptions of the approach, methods, tools and results are provided in Section 1 for HPOP, Section 2 for parameter and coordinate frame transformations, and Section 3 for access and visibility calculations. A short summary of the testing and results of each function is given below.

HPOP

The tests developed for the IV&V process systematically checked the accuracy of the HPOP's basic coordinate transformations, orbit propagation, and accumulation of perturbative forces for four different orbit types: geosynchronous orbit (GEO), highly elliptical orbit (HEO), medium Earth orbit (MEO), and low Earth orbit (LEO).

The J2000, Mean Equator, Mean Equinox (MEME) Earth-centered inertial / Earth-fixed transformation and propagation including only a spherical gravity model were compared to HPOP's basic coordinate transformations and orbit propagations. These results were treated as a baseline for comparison for the following tests, which included orbital perturbations.

Gravity, atmosphere, solar radiation pressure, and planetary perturbation models were tested individually for the different orbit types. After the propagation with each force model was independently evaluated, all of the force models listed above were incorporated into a single comprehensive test case for each orbit type.

Based on all of the test results, the differences between propagated orbit position (for periods ranging from one to seven days, depending on the orbit) between TRACE v2.4.9 and STK v4.1.0 ranged from sixteen centimeters or less for GEO, seven centimeters or less for HEO, twenty-one centimeters or less for LEO, to three centimeters or less for MEO. These small differences for the GEO, HEO, and MEO cases are probably differences in Greenwich hour angle, Jacchia-Roberts atmospheric density model for the HEO case, and/or different integration / interpolation / time tag schemes. For the LEO case, the differences are caused by the inclusion of the Jacchia-Roberts atmospheric model and solar radiation pressure model. While the LEO differences are larger than expected, the magnitudes are small for most applications, with the exception of those involving precision geodesy or altimetry work.

When two different programs integrate orbit trajectories, some differences are expected to occur due to different but equivalent algorithms or different but equivalent coding of algorithms. Each of these causes can result in differences that are attributed to numerical noise. That is, the differences just indicate the approximate level of accuracy that is obtainable for the particular calculations given the precision available from the computers used. In evaluating differences between HPOP and TRACE, effort was directed at determining when a difference was not due to numerical noise and trying to determine the cause. Several instances of non-numerical noise differences are noted and described in the results. We expect that for most users of HPOP, the differences will not be significant.

Parameter and Coordinate Frame Transformations

Validation consisted of comparing transformations of six orbit parameter sets in several coordinate frames with epochs spanning dates from 1986 to 2010—a total of 288 cases. Several near singular conditions, such as near zero eccentricity, and near zero and polar orbit plane inclinations, were validated for orbit parameter transformation. These scenarios, which ranged from low earth to supersynchronous (higher than GEO) orbits, were then exercised using the report feature of STK and the output captured to files. Each file represented the trajectory in eight orbit parameter sets and six coordinate reference frames. The agreement in computing satellite orbit parameters and coordinate transformations between the astrodynamics tools used at the Aerospace Corporation (TRACE v2.4.9, Rotate v1.0 and Geo v1.0) and STK v4.1.0 is excellent. In the areas of parameter and coordinate frame transformations the validation results identify STK as a tool for precision astrodynamics analyses at the decimeter level. Precision is established at a level of less than 12 centimeters for position and six millimeters per second for velocity transformations from inertial reference frames to an Earth-centered and fixed reference frame.

Access and Visibility Calculations

The validation of the access and visibility computations in STK v4.1.0 was completed by comparing data from 174 combinations of vehicles, sensors, and targets with results produced by similar programs developed by the Aerospace Corporation. Vehicle orbits included low-Earth circular orbits at four different inclinations, a highly elliptical orbit, and a geosynchronous orbit. Nine different sensor geometries were used, and access to two point targets and one area target were calculated. Twelve cases included satellite-to-satellite-to-ground station relays with and without range constraints. In the majority of cases (154), the results were almost identical, quite often to within 0.01%, in spite of differences in modeling philosophies and stressing cases designed to reveal such differences. Differences greater than 1% were observed in only 20 cases, all but one of which were found to match when minor variations in modeling of the Earth orientation parameters were taken into account. We have only one small unexplained difference for *one access* in one case, which will need to be addressed by AGI. The Aerospace Corporation is satisfied that the access and visibility computations in STK v4.1.0 are highly accurate and suitable for use in a broad range of typical space analysis applications.

1. High Precision Orbit Propagator

This section describes the Independent Validation and Verification (IV & V) tests performed on the High Precision Orbit Propagator (HPOP) used in the Satellite Tool Kit v4.1.0 (STK), a set of satellite analysis software tools developed by Analytical Graphics, Inc. The Aerospace Corporation's Trajectory Analysis and Orbit Determination Program v2.4.9 (TRACE) was used as the benchmark tool for conducting the tests.

The tests developed for the IV & V process systematically checked the accuracy of the HPOP's basic coordinate transformations, orbit propagation, and accumulation of perturbative forces for four different orbit types.

The J2000, Mean Equator, Mean Equinox (MEME) Earth-centered inertial / Earth-fixed transformation and propagation including only a spherical gravity model were compared to evaluate HPOP's basic coordinate transformations and orbit propagations. These results were treated as a baseline for comparison for the tests, which included orbital perturbations.

Gravity, atmosphere, solar radiation pressure, and planetary perturbation models were tested individually for the different orbit types. After the propagations with each force model were independently evaluated, all of the force models listed above were incorporated into a single comprehensive test case for each orbit type.

Based on all of the test results, the differences between propagated orbit position (for periods ranging from one to seven days, depending on the orbit) between TRACE v2.4.9 and STK v4.1.0 ranged from sixteen centimeters or less for GEO, seven centimeters or less for HEO, twenty-one centimeters or less for LEO, to three centimeters or less for MEO. These small differences for the GEO, HEO, and MEO cases are probably differences in Greenwich hour angle, Jacchia-Roberts atmospheric density model for the HEO case, and/or different integration / interpolation / time tag schemes. For the LEO case, the differences are caused by the inclusion of the Jacchia-Roberts atmospheric model and solar radiation pressure model. While the LEO differences are larger than expected, the magnitudes are small for most applications, with the exception of those involving precision geodesy or altimetry work.

1.1 Assumptions and Approach

The test orbits used to validate and verify HPOP include typical LEO, MEO, HEO, and GEO orbits, as outlined in Table 1.

Table 1. Test Orbit Initial States

	<u>LEO</u>	<u>MEO</u>	<u>HEO</u>	<u>GEO</u>
X	-14237.8 m	-1656.4 m	15854069.8 m	42283391.9 m
Y	6165158.3 m	10647065.8 m	14891698.9 m	0.000001485 m
Z	3559455.8 m	12688678.9 m	29783464.2 m	0.0000001300 m
x-dot	-7482.7 m/sec	-4905.6 m/sec	-1099.5 m/sec	-0.000000000108 m/sec
y-dot	-6.48 m/sec	-0.158 m/sec	1041.9 m/sec	3057.1 m/sec
z-dot	-3.74 m/sec	-0.188 m/sec	2083.8 m/sec	267.5 m/sec
<i>≈ Equivalent Keplerian Elements¹</i>				
A	7118918.7 m	16563894 m	26610257.5m	42241150.7 m
E	0.001	0.00005	0.7	0.001
I	30°	50°	63.435°	5°
Ω	0°	0°	0°	0°
ω	0°	0°	270°	180°
τ	-24.9 min	-88.4 min	-180.0 min	-720 min

Table 2 outlines the satellite effective areas, satellite weight, frequency of data output, and the duration of the test cases. The areas and weights do not correspond to particular satellites and were chosen to represent reasonable values for each orbit type.

Table 2. Test Case Orbit Parameters

Orbit Type	Satellite Effective Area (ft²)	Satellite Weight (lb)	Propagation Length (day)	Frequency Of Output (min)
LEO	20	200	1	1 minute
MEO	100	250	2	2 minutes
HEO	200	300	3	5 minutes
GEO	400	400	7	10 minutes

For all of the orbit types, 1 January 1998, 0:0:0 UTC was selected as epoch. The integration frame and time system was MEME of J2000 and UTC, respectively, since this frame and time system are commonly used in orbital analyses. Transformations between the Earth-centered inertial (ECI) and Earth-centered fixed (ECF) frames included the effects of precession, nutation, polar motion, and UT1-UTC corrections.

Prior to the validation process, closure tests were run for all of the orbit types to determine integrator step-size parameters required to provide the best TRACE integration for each type. Closure tests integrate the orbit equations of motion forward a finite amount of time, integrate the endpoint solution backward to the initial time, and compare the position and velocity over the time period of integration.

¹ semi-major axis (a), eccentricity (e), inclination (i), right ascension of the ascending node (Ω), argument of perigee (ω), minutes from midnight of epoch since last perigee passage (τ).

TRACE propagations including only a spherical gravity model were compared initially with equivalent propagations using STK. Upon successful completion of this comparison, gravity, atmosphere, solar radiation pressure, and planetary perturbation models were tested individually as outlined in Table 3.

Table 3. Force Models Applied to Orbit Types

Force	Force Model	Test Cases
Geopotential	WGS-84 EGM96	LEO, MEO, HEO, GEO
Planetary Effects	DE200	LEO, MEO, HEO, GEO
Solar Radiation Pressure	Flat Plate	LEO, MEO, HEO, GEO
Atmospheric Density	Jacchia-Roberts	LEO, HEO

After the propagations with each force model were independently evaluated, all the force models listed above were incorporated into a single test case for each orbit type. Test results were expressed as position, velocity, and acceleration differences in the Earth-centered inertial (ECI) and Earth-centered fixed (ECF) coordinate systems.

1.2 Results

This section presents the results of the TRACE closure tests, initial fundamental tests, and the final comprehensive tests.

1.2.1 TRACE Closure Tests

Closure tests were run for all of the orbit types to determine integrator step-size parameters required to provide the best TRACE integration for each type. Closure tests integrate the orbit equations of motion forward a finite amount of time, integrate the endpoint solution backward to the initial time, and compare the position and velocity over the time period of integration. Closure is accomplished if the differences in state at the initial time are below a given tolerance. The closure tests included the following force models: 70x70 WGS-84 EGM96 gravity, planetary perturbations, and solar radiation pressure.

TRACE integrator control parameters were selected such that closure test position state differences were a millimeter or less. These controls included integration step-size, frequency of perturbing force computation, and use of regularized time. Perturbing forces were computed at both the predictor and corrector steps of TRACE's predictor-corrector eighth-order, Gauss-Jackson differencing scheme. The maximum integrator step-size was set to 4, 1, and 0.25 minutes for the GEO, MEO, and LEO cases, respectively. Regularized time with 500 integration points per revolution was used for the HEO case.

1.2.2 Initial Tests

The J2000, MEME ECI / ECF transformation and propagations including only a spherical gravity model were compared as first steps in the validation process. Upon successful completion of this comparison, gravity, atmosphere, solar radiation pressure, and planetary perturbation models were tested individually. A qualitative summary of initial test results is presented in Table 4. Detailed numerical results of the initial tests are presented in the subsequent subsections.

Table 4. Qualitative Summary of Initial Test Results

<u>Test</u>	<u>Qualitative Results</u>
J2000, MEME ECI / EF Transformation	Millimeter level of position difference within an acceptable tolerance.
Spherical Gravity Model	Differences in Earth-fixed position and velocity appear to be due to apparent Greenwich hour angle differences, but the impact of apparent Greenwich hour angle differences seems to be within an acceptable tolerance.
WGS-84 EGM96 Gravity Model	Differences are on the order of the differences documented for the spherical gravity model tests.
Celestial Perturbation Model	Differences are on the order of the differences documented for the spherical gravity model tests.
Solar Radiation Pressure Model	Differences are of the same order of magnitude as differences documented for the spherical gravity model propagations, with the exception of the LEO case. LEO differences appear to result from STK and TRACE usage of different eclipse calculations.
Jacchia-Roberts Atmospheric Density Model	Test differences are larger than differences documented for the spherical gravity model tests, and no obvious cause was found for the discrepancies. However, the differences are small for most applications, with the exception of those involving precision geodesy or altimetry work.

1.2.2.1 Transformation between J2000, MEME ECI and ECF

This initial analysis involved converting the test case initial states in J2000 MEME ECI to ECF coordinates using TRACE and STK and comparing the results. The ECF position differences for the orbit types are listed in Table 5.

Table 5. TRACE v2.4.9 - STK v4.1.0 ECF Position Differences

Orbit	x (m)	y (m)	z (m)
GEO	-1.190E-04	1.150E-05	-4.642E-03
HEO	-5.136E-05	-4.718E-05	1.317E-05
LEO	-2.516E-06	-2.056E-05	1.754E-06
MEO	-4.781E-06	-3.610E-05	5.676E-06

The millimeter or less level of position difference is within an acceptable tolerance.

1.2.2.2 Spherical Gravity Model Tests

TRACE propagations using a spherical gravity model were compared with equivalent STK propagations. Table 6 shows the maximum position, velocity, and acceleration TRACE - STK differences over the propagation length for the orbit types.

Table 6. Spherical Gravity Model Tests - Maximum TRACE v2.4.9 – STK v4.1.0 Differences

Orbit	Propagation Length (days)	Position (m)	Velocity (m/sec)	Acceleration (m/sec²)
<i>ECI Frame</i>				
GEO	7	0.0552	4.01E-6	6.42E-6
HEO	3	0.00698	4.51E-6	0.0169
LEO	1	0.000317	3.23E-7	1.63E-6
MEO	2	0.000607	1.82E-7	3.83E-7
<i>ECF Frame</i>				
GEO	7	0.122	0.00249	6.01E-7
HEO	3	0.0375	0.00353	0.0169
LEO	1	0.0104	0.000509	1.55E-6
MEO	2	0.0241	0.00119	3.59E-7

The high acceleration difference for the HEO orbit occurs only when the satellite is at or near perigee. The observed acceleration differences are probably due to usage of different integration / interpolation / time tag schemes.

The ECF position differences are larger than expected. After ruling out precession, nutation, pole, and UT1 offsets, these differences in Earth-fixed position and velocity appear to be due to apparent Greenwich hour angle differences, on the order of 1.5E-9 radians. Given the available information, no obvious cause was found for the TRACE and STK apparent Greenwich hour angle discrepancies. However, the impact of apparent Greenwich hour angle differences seems to be within an acceptable tolerance.

1.2.2.3 WGS-84 EGM96 70x70 Gravity Model Tests

TRACE propagations using WGS-84 EGM96 70x70 gravity model were compared with equivalent STK propagations. Table 7 shows the maximum position, velocity, and acceleration TRACE - STK differences over the propagation length for the orbit types.

Table 7. WGS-84 EGM96 Gravity Model Tests - Maximum TRACE v2.4.9 – STK v4.1.0 Differences

Orbit	Propagation Length (days)	Position (m)	Velocity (m/sec)	Acceleration (m/sec²)
<i>ECI Frame</i>				
GEO	7	0.0552	4.01E-6	6.42E-6
HEO	3	0.00694	4.48E-6	0.0166
LEO	1	0.000280	3.12E-7	1.12E-5
MEO	2	0.000608	1.82E-7	3.83E-7
<i>ECF Frame</i>				
GEO	7	0.122	0.00249	6.01E-7
HEO	3	0.0375	0.00353	0.0166
LEO	1	0.0104	0.00051	1.14E-5
MEO	2	0.0241	0.00119	3.59E-7

The maximum ECI and ECF position differences are of the same order of magnitude as the differences documented for the spherical gravity model propagations, and the larger ECF differences probably result from discrepancies in apparent Greenwich hour angle.

1.2.2.4 Celestial Perturbations Tests

TRACE propagations using solar and lunar perturbations were compared with equivalent STK propagations; both programs utilized the JPL DE200 file for Sun and Moon positions. Table 8 shows the maximum position, velocity, and acceleration TRACE - STK differences over the propagation length for the orbit types.

Table 8. Celestial Perturbations Tests - Maximum TRACE v2.4.9 – STK v4.1.0 Differences

Orbit	Propagation Length (days)	Position (m)	Velocity (m/sec)	Acceleration (m/sec²)
<i>ECI Frame</i>				
GEO	7	0.0743	5.39E-6	6.42E-6
HEO	3	0.0130	8.28E-6	0.0168
LEO	1	0.000296	2.98E-7	1.63E-6
MEO	2	0.000449	1.27E-7	3.83E-7
<i>ECF Frame</i>				
GEO	7	0.141	0.00249	6.02E-7
HEO	3	0.0379	0.00353	0.0168
LEO	1	0.0103	0.000509	1.55E-6
MEO	2	0.0239	0.00119	3.59E-7

The maximum ECI and ECF position differences are of the same order of magnitude as the differences documented for the spherical gravity model propagations, and the larger EF differences probably result from discrepancies in apparent Greenwich hour angle.

1.2.2.5 Solar Radiation Pressure Model Tests

TRACE propagations using the flat plate solar radiation pressure model were compared with equivalent STK propagations; both programs use apparent Sun coordinates for solar radiation pressure calculations. Table 9 shows the maximum position, velocity, and acceleration TRACE - STK differences over the propagation length for the orbit types.

Table 9. Solar Radiation Pressure Model Tests - Maximum TRACE v2.4.9 – STK v4.1.0 Differences

Orbit	Propagation Length (days)	Position (m)	Velocity (m/sec)	Acceleration (m/sec ²)
<i>ECI Frame</i>				
GEO	7	0.0695	5.05E-6	6.42E-6
HEO	3	0.00822	5.36E-6	0.0169
LEO	1	0.202	0.000218	1.50E-6
MEO	2	0.000443	1.27E-7	3.83E-7
<i>ECF Frame</i>				
GEO	7	0.136	0.00249	6.01E-7
HEO	3	0.0375	0.00353	0.0169
LEO	1	0.210	0.000541	1.42E-6
MEO	2	0.0240	0.00119	3.59E-7

The maximum TRACE - STK differences are of the same order of magnitude as differences documented for the spherical gravity model propagations, with the exception of the LEO case. For the LEO case, both TRACE and STK apply a scale factor to the solar radiation pressure force. This factor corresponds to the estimated fraction of light visible to the spacecraft during the penumbra eclipse stage. Differences in integration steps will produce slightly different eclipse scale factors. Thus, the LEO differences probably result from STK and TRACE usage of different eclipse calculations.

1.2.2.6 Jacchia-Roberts Atmospheric Density Model Tests

TRACE propagations using the Jacchia-Roberts atmospheric density model were compared with equivalent STK propagations; both programs use true Sun coordinates for atmospheric density calculations. Table 10 shows the maximum position, velocity, and acceleration TRACE - STK differences over the propagation length for the orbit types.

Table 10. Atmospheric Density Model Tests - Maximum TRACE v2.4.9 – STK v4.1.0 Differences

Orbit	Propagation Length (days)	Position (m)	Velocity (m/sec)	Acceleration (m/sec ²)
<i>ECI Frame</i>				
HEO	3	0.0616	4.16E-5	0.0169
LEO	1	0.0621	6.76E-5	1.59E-6
<i>ECF Frame</i>				
HEO	3	0.0655	0.00353	0.0169
LEO	1	0.0706	0.00051	1.51E-6

The maximum ECI and ECF position differences are larger than the differences documented for the spherical gravity model propagations. Given the available information, no obvious cause was found for the TRACE and STK Jacchia-Roberts test result discrepancies. However, the differences are small for most applications, with the exception of those involving precision geodesy or altimetry work.

1.2.3 Comprehensive Tests

After the propagations with each force model were independently evaluated, all of the force models tested individually were incorporated into a single comprehensive test case for each orbit type (See Table 3). TRACE propagations of the comprehensive test cases were compared with equivalent STK propagations. Table 11 shows the maximum position, velocity, and acceleration TRACE - STK differences over the propagation length for the orbit types.

Table 11. Comprehensive Tests - Maximum TRACE v2.4.9 – STK v4.1.0 Differences

Orbit	Propagation Length (days)	Position (m)	Velocity (m/sec)	Acceleration (m/sec ²)
<i>ECI Frame</i>				
GEO	7	0.0886	6.44E-6	6.42E-6
HEO	3	0.0625	4.23E-5	0.0166
LEO	1	0.0540	5.49E-5	1.12E-5
MEO	2	0.000273	7.96E-8	3.83E-7
<i>ECF Frame</i>				
GEO	7	0.155	0.00249	6.02E-7
HEO	3	0.0654	0.00353	0.0166
LEO	1	0.0628	5.10E-4	1.14E-5
MEO	2	0.0238	0.00119	3.59E-7

For the GEO and MEO cases, the maximum TRACE - STK ECI position and velocity are of the same order of magnitude as the differences documented for the spherical gravity model propagations. Part of the ECF difference is due to differences in the J2000 ECI / ECF transformation resulting from apparent Greenwich hour angle discrepancies.

For the HEO and LEO cases, the maximum TRACE - STK position and velocity differences are caused by inclusion of the Jacchia-Roberts atmospheric density model. Inclusion of the solar radiation pressure model contributed some additional error to the LEO test case results. However, the differences are small for most applications, with the exception of those involving precision geodesy or altimetry work.

1.3 Conclusions

The tests developed for the IV & V process systematically checked the accuracy of the HPOP's basic coordinate transformations, orbit propagation, and accumulation of perturbative forces for four different orbit types.

The J2000, MEME ECI / ECF transformation and propagation including only a spherical gravity model were compared to evaluate HPOP's basic coordinate transformations and orbit propagations. The observed Earth-fixed position and velocity differences from these propagations appear to be due to apparent Greenwich hour angle differences, but the impact of apparent Greenwich hour angle differences

seems to be within an acceptable tolerance. These results were treated as a baseline for comparison for the tests, which included orbital perturbations.

Gravity, atmosphere, solar radiation pressure, and planetary perturbation models were tested individually for the different orbit types. The results of these tests are as follows:

1. Gravity model and celestial perturbations test results are of the same order of magnitude as the results documented for the spherical gravity model propagations, and the observed Earth-fixed position and velocity differences probably result from discrepancies in apparent Greenwich hour angle.
2. Solar radiation pressure model tests resulted in maximum TRACE - STK differences of the same order of magnitude as differences documented for the spherical gravity model propagations, with the exception of the LEO case. LEO differences appear to result from STK and TRACE usage of different eclipse calculations.
3. Jacchia-Roberts atmospheric density tests resulted in larger maximum ECI and ECF position differences than the differences documented for the spherical gravity model propagations, and no obvious cause was found for the discrepancies.

The comprehensive tests involved all of the models tested individually. For the GEO and MEO cases, the maximum TRACE - STK ECI position and velocity are of the same order of magnitude as the differences documented for the spherical gravity model propagations. For the HEO and LEO cases, the maximum TRACE - STK position and velocity differences are caused by inclusion of the Jacchia-Roberts atmospheric density model. Inclusion of the solar radiation pressure model contributed some additional error to the LEO test case results.

While larger than expected differences were found for tests involving Jacchia-Roberts atmospheric density and solar radiation pressure for which eclipsing is estimated, the differences are small for most applications, with the exception of those involving precision geodesy or altimetry work.

2. Parameter and Coordinate Frame Transformations

This section describes the validation of STK, Version 4.1.0, with respect to parameter and coordinate frame transformations. Validation consisted of preparing six orbit parameter sets in several coordinate frames with epochs spanning dates from 1986 to 2010 in the STK scenario database. Several near singular conditions, such as near zero eccentricity, and near zero and polar orbit plane inclinations, were validated for orbit parameter transformation. These scenarios were then exercised using the STK report feature and the output captured to files. Each file represented the trajectory in eight orbit parameter sets and six coordinate reference frames. The agreement between the astrodynamics tools used at The Aerospace Corporation (TRACE v2.4.9, Rotate v1.0 and Geo v1.0) and STK v4.1.0 is excellent. In the areas of parameter and coordinate frame transformations, the validation results identify STK as a tool for precision astrodynamics analyses at the decimeter level. Precision is established at a level of less than 12 centimeters for position and six millimeters per second for velocity transformations from inertial reference frames to an Earth-centered and fixed reference frame.

2.1 Methodology

The validation of STK for parameter and reference frame transformations is performed through six procedures that may be executed individually via a PERL script or as a set by means of a shell script. The scripts are executed under a UNIX operating system. An overview of the tools and databases is provided later in this section. Since the STK scenarios, data files output by the astrodynamics tools of The Aerospace Corporation, and PERL scripts are all deliverable along with this report, a discussion of the organization of that data is also provided. Later in this section, the validation strategy, scope and limitations are discussed, the results of each validation procedure are given, and validation results are summarized.

Validation consisted of preparing six orbit parameter sets in several coordinate frames with epochs spanning dates from 1986 to 2010 in the STK scenario database. Several near singular conditions, such as near zero eccentricity, and near zero and polar orbit plane inclinations, were validated for orbit parameter transformation. These scenarios were then exercised using the STK report feature and the output captured to files. Each file represented the trajectory in eight orbit parameter sets and six coordinate reference frames. Table 12 lists the orbit parameter sets and reference frames for which validation was performed.

Table 12. Validation Output Matrix

Reference Frames Output	Orbit Parameter Set Output
MEME, J2000	Cartesian
MEME, B1950	Classical (Keplerian)
TETE of Epoch	Equinoctial
TETE of Date	Geocentric Spherical
TEME of Date	Geodetic Spherical
ECF	Mixed Spherical
	LLR and LLA

2.2 Tools and Databases

The Aerospace Corporation astrodynamic tools used for the validation of STK parameter and reference frame transformations include TRACE, Rotate, and Geo. The input and output data files of these computer programs are deliverable. The executable programs Geo and Rotate, targeted for an SGI Indigo 2 computer, will also be delivered; however, they will not be required to execute the validation tests. The PERL script is platform-independent; however, it does use commands that are associated with a Bourne or Korn shell script. The Connect interface program was provided by AGI and must be compiled and linked for platforms other than an SGI.

2.2.1 Databases

The input to STK is in the directory stk41. The file names are v1 through v6. The output from STK is stored along with the output from TRACE, Rotate, and Geo in the directory stk41/data. The input to TRACE, Rotate, and Geo are stored in the directories stk41/Trace, stk41/Rotate, and stk41/geoc2geod. The PERL scripts are stored in directory stk41/scripts. Finally, the “c” program that provides the Connect interface is located at stk41/stk.connect/AGIPCExp. Its input files are stored in the directory stk41/data. In all cases input or output files for a validation procedure begin with the two character identifier for the procedure (i.e. v1, v2, ...). Input files have the suffix “.in” and output files have the suffix “.out”. PERL script file names have the suffix “.perl” and shell script file names end in “.csh”.

2.2.2 Scripts

There are three PERL scripts in the directory stk41/scripts. Two are utility scripts and the other, as the name suggests, is the validation script. The validation script must be executed from the stk41 directory. The command line is: “ scripts/validate.perl v?”, where the ? represents the case number 1 through 6.

The shell script “run_all.csh” is located in the stk41 directory. It will execute all six validation cases.

2.2.3 Geo

The computer program “geo” is located in the directory stk41/geoc2geod. Its function is to compute geodetic latitude and altitude from an input Earth fixed position. The delivered version of the PERL scripts will not execute Geo, but will access data that it outputs. The line of code in the script that would execute Geo will begin with a “#” so it can easily be reactivated.

2.2.4 Rotate

The computer program Rotate is located in directory stk41/Rotate. Its function for this validation effort is to transform an Earth fixed position and velocity state vector to the TrueEquatorMeanEquinox of date reference frame. The PERL script does not execute Rotate directly but accesses its output file. The executable program is located in stk41/Rotate/rotate.

2.2.5 TRACE

The computer program TRACE is stored as a system utility and its executable code is not available in the stk41 directory, which is deliverable. Its input and output files are located in the directory stk41/Trace. The PERL script accesses the TRACE output files in the directory stk41/data. All data generated by Aerospace tools—with the exception of transformations involving the TEME reference frame and geodetic parameters—were produced by TRACE.

2.2.6 Physical Constants

The physical constants used for the reference frame and parameter transformation validation tests are derived from the World Geodetic System 1984 (EGM 96). The fundamental parameters are listed in Table 13.

Table 13. Physical Constants

Parameter	Magnitude
Earth's gravitational constant (mass of the earth's atmosphere included)	$3986004.418 \times 10^8 \text{ m}^3/\text{s}^2$
Earth's semi-major axis	6378137.0 meters
Earth's semi-minor axis	6356752.3142 meters
Angular velocity of the earth in a precessing reference frame	$(7292115.8553 \times 10^{-11} + 4.3 \times 10^{-15} \text{tu})$ radians/second where tu is Julian centuries from epoch j2000.0

2.3 Validation Procedures

There are six validation procedures, v1 through v6, each of which varies the orbit type and input reference frame. Table 14 provides a top level view of the input conditions of each of the procedures. The output orbit parameter sets and reference frames, listed in Table 12 above, are the same for all six procedures. The classical elements of each of the six orbits are provided in Table 15.

Table 14. Validation Input Matrix

Orbit Class	Reference Date and Time	Reference Frames Input	Parameters Input	Special Conditions
Low Earth Orbit (LEO)	4 October 1994 16:20:30.000	TETE of Epoch (Instant)	Classical	Polar Orbit
GPS Orbit (GPS)	2 February 1998 12:25:15.000	J2000	Cartesian	
High Eccentricity Orbit (HEO)	10 September 1993 00:00:00.000	TEME Midnight of Epoch Date	Cartesian	
Medium Earth Orbit (MEO)	1 April 1986 2:12:12.000	TETE of Epoch (Instant)	Classical	Retrograde
Geosynchronous Earth Orbit (GEO)	1 December 2000 18:23:58.410	J2000	Cartesian	Near Zero Inclination
Super-GEO (SEO)	25 December 2010 9:51:42.900	J2000	Cartesian	Near Zero Eccentricity

Table 15. Orbital Elements (Meters, Degrees)

Case	Semi-major Axis	Eccentricity	Inclination	RAAN	Argument of Perigee	True Anomaly
v1	7136635.001	0.00349497	90.01109	0.8383513	260.51023	0.18307E-5
v2	26559731.751	0.00355145	54.65840	183.78063	282.99106	22.203747
v3	24275976.824	0.72783306	26.51974	214.33883	179.12005	189.53880
v4	8600537.001	0.10000000	98.79267	0.8520010	260.51435	44.500000
v5	42164387.803	0.00024265	0.001	69.744936	270.40855	203.97827
v6	42560851.827	9.89152E-5	8.9118209	51.354771	207.21330	135.65626

2.3.1 Reference Frames

The reference frame tests consist of six procedures. Each has a different coordinate frame year and time of day. They evaluate transformations corresponding to an epoch date, and coordinate epochs (in addition to J2000). These tests also evaluate the proper handling of the leap second used to determine UTC (Coordinated Universal Time) from TAI (International Atomic Time). Notice that the reference dates selected in Table 14 result in an extensive evaluation of the reference time transformation algorithm of STK.

2.3.2 Orbit Parameter Sets

The orbit parameter set validation consists of six procedures that evaluate the orbit classes (LEO, GPS, HEO, MEO, GEO, SEO). It includes singularity testing for near zero eccentricity and inclination, near 90 degree inclination, and retrograde orbits.

Only the Cartesian and mixed spherical orbit parameter sets are defined in the Earth-fixed frame.

2.3.3 Earth-Fixed Transformations

The transformation from the inertial reference frames (J2000, B1950, MEME, True Equator and Mean Equinox [TEME], True Equator and True Equinox [TETE]) to the Earth-fixed reference frame (ECF) is very arcane but relative simple to follow. Beginning at the mean equator and mean equinox reference frame the precession and nutation transformations must be applied to get a parameter set defined in the true equator and true equinox reference frame. Then the nutation in longitude must be computed and applied to get to the true equator and mean equinox reference frame. Finally the sidereal rotation angle is computed to get to an Earth-fixed reference frame. If a very accurate Earth-fixed vector is required the seasonally dependent correction to UT2 is applied, then the unpredictable correction is applied to get to UT1. Finally a pole wander correction is applied. (If the UT1 correction is derived from the tables transmitted by the US Naval Observatory, the UT2 correction must not be separately applied, since it is included in the tables.)

2.3.4 Earth Orientation Parameters

The EOP file used by STK for the validation procedures is EOP.dat.7_Feb_00. It was created by merging the EOP.dat and EOP.dat.1976 files. The parameters used by TRACE and Rotate were also taken from that file. The accuracy of the transformations that use the correction to UTC (i.e., DUT1) and pole wander is obviously dependent upon the accuracy of the parameters in that table.

When the date of a vector is outside the span of the EOP.dat table, STK uses the last (or first) entry in that table for the DUT1 and pole wander parameters. That was done to avoid discontinuities in the model. Since the correct values of those parameters are unknown after the last entry in the table and precision ephemerides are unlikely to be required for times prior to 1976, the TRACE and Rotate parameters were modeled in the same way for the validation cases.

2.3.5 Validation Environment

The computer environment under which the validation was performed is a workstation with a UNIX operating system and a TCP/IP Network connectivity. An SGI system was used with an IRIX 6.5 Operating System. It was used to execute the Satellite Tool Kit (Version 4.1.0), Rotate (Version 1.0), Geo (Version 1.0), and PERL (4.0.1.3). TRACE (Release 2.4.9) was executed on a SUN system. The scripts to be delivered with this report will use the output files from TRACE, Rotate, and Geo. It should be possible to execute the PERL scripts on any platform with a UNIX operating system.

2.3.6 Validation Limitations

Two aspects of STK in areas that correspond to parameter and reference frame transformations were not validated directly. These include the parameter transformations from (or to) Delaunay variables and those rate terms associated with the Earth's longitude, latitude, and altitude or radial distance. Not directly validated are transformations internal to the Graphical User Interface (GUI).

The reference frames TrueEquatorTrueEquinox of date and TrueEquatorMeanEquinox of epoch are not commonly used; therefore they are validated only at the time of day where they correspond to the TrueEquatorTrueEquinox of epoch (TETE) and TrueEquatorMeanEquinox of date (TEME).

The B1950/FK4 transformations were validated only for Cartesian position and velocity state vector transformations from an ECF frame to the B1950/FK4 MEME frame. The decision to limit this validation was based upon the fact that the B1950/FK4 reference frame is rarely used. It has been supplanted by the J2000/FK5 system.

2.4 Validation Results

A summary of the validation results is presented for each of six cases. They represent the differences between the data generated by Aerospace Corporation tools and those produced by STK. A discussion of the results is provided along with the data. As previously discussed, where The Aerospace Corporation does not have a tool which produces a particular transformation output by STK, the parameters corresponding to that transformation have been ignored. The Aerospace Corporation astrodynamics tools that were used for the validation were discussed previously.

The complete output of the validation procedures is provided in Tables 16 through 21. The format and contents of these tables are taken directly from the output files of the validation procedures (v1 through v6). Sections 2.4.1 through 2.4.6 below summarize in tabular format the significant findings from each of the complete tables. The reader is cautioned that some comparisons identify level of agreement, while others identify levels of difference.

Some comments are generic to all test cases:

The B1950/FK4 total position and velocity agree to the levels cited above. The discrepancy in the individual components is due to a rotation difference. The component errors will increase as a function of distance from the geocenter. Equinoctial elements in general agree to more than six significant digits after the decimal point.

2.4.1 Validation Case 1 – LEO Orbit

Attribute	Position	Velocity
Complete Difference Table	Table 16	
General Cartesian Agreement	8 Millimeters	3 Microns/Second
Exception: ECF Differences	8 Millimeters	5 Millimeters/Second
Orbital Eccentricity and Angular Agreement	Better than 1×10^{-6}	
Equinoctial Element Agreement	Better than 1×10^{-6} , except semi-major axis (0.4 millimeter)	

This nearly polar orbit establishes the capability of STK to process trajectories with that characteristic.

2.4.2 Validation Case 2 – GPS Orbit

Attribute	Position	Velocity
Complete Difference Table	Table 17	
General Cartesian Agreement	3 Centimeters	Micron/Second
Exception: ECF Differences	7 Millimeters	Millimeter/Second
Orbital Eccentricity and Angular Agreement	Better than 1×10^{-6}	
Equinoctial Element Agreement	Better than 1×10^{-6} , except semi-major axis (4 millimeters)	

The MEME, J2000 positions and velocities agree perfectly for at least eight significant digits after the decimal point (i.e., $<1 \times 10^{-8}$ meters and $<1 \times 10^{-8}$ m/second.) This agreement is due to the fact that the STK input is in the MEME, J2000 reference frame and the TRACE output has 14 significant digits.

2.4.3 Validation Case 3 – HEO Orbit

Attribute	Position	Velocity
Complete Difference Table	Table 18	
General Cartesian Agreement	2 Centimeters	Micron/Second
Exception: ECF Differences	2 Centimeters	2 Millimeters/Second
Orbital Eccentricity and Angular Agreement	Better than 1×10^{-6}	
Equinoctial Element Agreement	Complete agreement' except for semi-major axis where agreement is better than 1×10^{-6}	

The MEME, J2000 positions and velocities agree perfectly for at least eight significant digits after the decimal point. This agreement is due to the fact that, although the STK input is TEME of date, the TRACE input, taken from the STK output, is in the MEME, J2000 reference frame. Also the TRACE output vector has 14 significant digits for this reference frame.

Validation Case 4 – MEO Orbit

Attribute	Position	Velocity
Complete Difference Table	Table 19	
General Cartesian Agreement	2 Centimeters	0.1 Millimeter/Second
Exception: ECF Differences	2 Centimeters	0.4 Millimeter/Second
Orbital Eccentricity and Angular Agreement	Better than 1×10^{-6}	
Equinoctial Element Agreement	Better than 1×10^{-6}	

The retrograde orbit establishes the capability of STK to process trajectories with that characteristic.

2.4.5 Validation Case 5 – GEO Orbit

Attribute	Position	Velocity
Complete Difference Table	Table 20	
General Cartesian Agreement	12 Centimeters	Micron/Second
Exception: ECF Differences	6 Centimeters	6 Millimeters/Second
Orbital Eccentricity and Angular Agreement	Better than 1×10^{-6} , except argument of perigee (0.02 millidegrees)	
Equinoctial Element Agreement	Better than 1×10^{-6} , except semi-major axis (9 millimeter)	

The MEME, J2000 positions and velocities agree perfectly for at least eight significant digits after the decimal point. This agreement is due to the fact that, although the STK input is TEME of date, the TRACE input, taken from the STK output, is in the MEME, J2000 reference frame. Also the TRACE output vector has 14 significant digits for this reference frame. This near zero inclination (0.001 degrees) case establishes the validity of the STK parameter transformations near this singularity point.

2.4.6 Validation Case 6 – SEO Orbit

Attribute	Position	Velocity
Complete Difference Table	Table 21	
General Cartesian Agreement	5 Centimeters	4 Microns/Second
Exception: ECF Differences	12 Centimeters	5 Millimeter/Second
Orbital Eccentricity and Angular Agreement	Better than 1×10^{-6}	
Equinoctial Element Agreement	Better than 1×10^{-6} , except semi-major axis (6 microns)	

The MEME, J2000 positions and velocities agree perfectly for at least eight significant digits after the decimal point. This agreement is due to the fact that the STK and the TRACE input are identical and expressed in the MEME, J2000 reference frame. Also the TRACE output vector has 14 significant digits for this reference frame. This near zero eccentricity case establishes the validity of the STK parameter transformations near this singularity point.

Table 16. Case v1

Test v1: Parameter differences in the sense Aerospace - STK
 LEO, Epoch at 4 Oct 1994, 16:20:30.000000
 Difference are in units of meters, meters/second, and degrees.

TETE of Date (x,y,z,xd,yd,zd):	-0.00070000	-0.00814562	-0.00004790	0.00000004	-0.00000246	-0.00000070
TETE of Epoch (x,y,z,xd,yd,zd):	-0.00070000	-0.00814562	-0.00004790	0.00000004	-0.00000246	-0.00000070
TEME of Date (x,y,z,xd,yd,zd):	-0.00034160	-0.00718352	-0.00000720	0.00000028	0.00000204	-0.00000100
ECF (x,y,z,xd,yd,zd):	0.00809794	0.00261690	0.00018160	-0.00051844	0.00017792	-0.00004716
MEME - B1950 (x,y,z,xd,yd,zd):	0.51701560	1.25855871	-0.08994160	0.00009662	-0.00056323	0.00054991
(r,v):	0.00047892	-0.00000002				
MEME - J2000 (x,y,z,xd,yd,zd):	-0.00035450	-0.00605865	-0.00029130	-0.00000035	-0.00000262	-0.00000081
MEME J2000 (a,e,i,raan,arg_perigee,ta):	0.00034960	-0.00000003	0.00000002	0.00000027	-0.00000037	-0.00000017
MEME J2000 (ma,arg_lat,apogee_ht,apogee_per_ht,perigee):	-0.00000018	0.00000047	-0.00512433	-0.00512433	-0.00628563	-0.00628563
MEME J2000 (mean motion, ea, tau, kepl_period):	0.0000000016	-0.00000018	0.00000230	0.00000009		
MEME J2000 (a,ag,af,chi,psi,mean long):	0.00034960	0.000000000	0.000000000	-0.000000001	-0.000000001	-0.00000001
LLR - J2000 (dec,ra,r):	-0.000000048	-0.000000199	-0.00020			
Mixed Spherical, MEME - J2000 (geodetic lat,lon,alt,hfpa,az,v):	0.000000219	0.000000426	0.000264896	0.000000006	-0.000000270	0.000000254
Spherical, MEME-J2000 (ra,dec,rad,hfpa,azimuth,velocity):	-0.000000199	-0.000000048	-0.000199299	0.000000006	-0.000000270	0.000000254
LLA, ECF (geodetic lat,lon,alt):	0.000000219	0.000000426	0.000264896			
LLR, ECF (lat,lon,r):	-0.000000110	0.000000426	-0.000199299			

Table 17. Case v2

Test v2: Parameter differences in the sense Aerospace - STK
 GPS, Epoch at 2 Feb 1998, 12:25:15.000000
 Difference are in units of meters, meters/second, and degrees.

TETE of Date (x,y,z,xd,yd,zd):	0.00177000	0.00889500	0.00364700	0.00000016	0.00000205	0.00000092
TETE of Epoch (x,y,z,xd,yd,zd):	0.00177000	0.00889500	0.00364700	0.00000016	0.00000205	0.00000092
TEME of Date (x,y,z,xd,yd,zd):	0.01238200	0.02597200	0.00585400	-0.00000216	0.00000506	0.00000133
ECF (x,y,z,xd,yd,zd):	-0.00349000	-0.00695760	0.00485400	-0.00106178	-0.00003881	0.00118837
MEME - B1950 (x,y,z,xd,yd,zd):	9.01555300	3.51453300	-5.88127900	-0.00097806	0.00030114	-0.00140654
(r,v):	0.00018345	-0.00000026				
MEME - J2000 (x,y,z,xd,yd,zd):	0.00000000	0.00000000	0.00000000	0.00000000	0.00000000	0.00000000
MEME J2000 (a,e,i,raan,arg_perigee,ta):	-0.00401700	0.00000045	-0.00000011	-0.00000039	-0.00000080	-0.00000003
MEME J2000 (ma,arg_lat,apogee_ht,apogee,per_ht,perigee):	0.00000042	0.00000017	-0.03142047	-0.03142047	-0.02191074	-0.02191075
MEME J2000 (mean motion, ea, tau, kepl_period):	-0.0000000007	0.00000044	0.00004575	-0.00000933		
MEME J2000 (a,ag,af,chi,psi,mean long):	-0.00401700	-0.000000001	0.000000000	0.000000000	0.000000000	0.00000001
LLR - J2000 (dec,ra,r):	0.000000129	0.000000013	0.00054			
Mixed Spherical, MEME - J2000 (geodetic lat,lon,alt,hfpa,az,v):	0.000000505	-0.000000151	-0.000195388	0.000000458	0.000000476	-0.000000106
Spherical, MEME-J2000 (ra,dec,rad,hfpa,azimuth,velocity):	0.000000013	0.000000129	0.000540998	0.000000458	0.000000476	-0.000000106
LLA, ECF (geodetic lat,lon,alt):	0.000000505	-0.000000151	-0.000195388			
LLR, ECF (lat,lon,r):	-0.000000445	-0.000000151	0.000540998			

Table 18. Case v3

Test v3: Parameter differences in the sense Aerospace - STK
 HEO, Epoch at 10 Sep 1993, 0:0:0.000000
 Difference are in units of meters, meters/second, and degrees.

TETE of Date (x,y,z,xd,yd,zd):						
0.01562900	-0.01897400	-0.01156940	0.00000038	0.00000128	-0.00000002	
TETE of Epoch (x,y,z,xd,yd,zd):						
0.01562900	-0.01897400	-0.01156940	0.00000038	0.00000128	-0.00000002	
TEME of Date (x,y,z,xd,yd,zd):						
0.01115600	-0.01267500	-0.00817910	-0.00000008	0.00000073	0.00000002	
ECF (x,y,z,xd,yd,zd):						
0.01401300	-0.01132900	-0.01118390	0.00032121	-0.00009895	0.00169414	
MEME - B1950 (x,y,z,xd,yd,zd):						
-2.79423700	2.62294400	-5.02087660	-0.00013777	-0.00017943	0.00015421	
(r,v):						
0.00015577	0.00000017					
MEME - J2000 (x,y,z,xd,yd,zd):						
0.00000000	0.00000000	0.00000000	0.00000000	0.00000000	0.00000000	
MEME J2000 (a,e,i,raan,arg_perigee,ta):						
0.00000100	0.00000006	-0.00000042	-0.00000036	0.00000045	-0.00000019	
MEME J2000 (ma,arg_lat,apogee_ht,apogee,per_ht,perigee):						
0.00000023	0.00000026	-0.03597306	-0.03597306	-0.00551040	-0.00551040	
MEME J2000 (mean motion, ea, tau, kepl_period):						
-0.0000000014	-0.00000003	0.00000051	-0.00000024			
MEME J2000 (a,ag,af,chi,psi,mean long):						
0.00000100	0.00000000	0.00000000	0.00000000	0.00000000	0.00000000	
LLR - J2000 (dec,ra,r):						
0.000000395	-0.000000182	0.00023				
Mixed Spherical, MEME - J2000 (geodetic lat,lon,alt,hfpa,az,v):						
0.000000106	-0.000000352	0.000405274	0.000000481	-0.000000317	-0.000000357	
Spherical, MEME-J2000 (ra,dec,rad,hfpa,azimuth,velocity):						
-0.000000182	0.000000395	0.000231996	0.000000481	-0.000000317	-0.000000357	
LLA, ECF (geodetic lat,lon,alt):						
0.000000106	-0.000000352	0.000405274				
LLR, ECF (lat,lon,r):						
-0.000000043	-0.000000352	0.000231996				

Table 19. Case v4

Test v4: Parameter differences in the sense Aerospace - STK
 MEO, Epoch at 1 Apr 1986, 2:12:12.000000
 Difference are in units of meters, meters/second, and degrees.

TETE of Date (x,y,z,xd,yd,zd):						
-0.00106750	0.01294720	0.00210600	0.00000004	0.00001509	0.00000280	
TETE of Epoch (x,y,z,xd,yd,zd):						
-0.00106750	0.01294720	0.00210600	0.00000004	0.00001509	0.00000280	
TEME of Date (x,y,z,xd,yd,zd):						
0.00015600	0.00634680	0.00199780	-0.00000041	0.00000880	0.00000300	
ECF (x,y,z,xd,yd,zd):						
-0.01001020	-0.01483970	0.00248370	-0.00032850	0.00008123	0.00023707	
MEME - B1950 (x,y,z,xd,yd,zd):						
0.65791070	-0.02793200	0.46665840	-0.00038822	-0.00006919	0.00063272	
(r,v):						
-0.00092303	0.00000036					
MEME - J2000 (x,y,z,xd,yd,zd):						
-0.00551730	0.00097070	-0.00342470	0.00000351	0.00000019	-0.00000464	
MEME J2000 (a,e,i,raan,arg_perigee,ta):						
-0.00000040	0.00000000	0.00000018	0.00000002	0.00000004	-0.00000004	
MEME J2000 (ma,arg_lat,apogee_ht,apogee,per_ht,perigee):						
0.00000032	0.00000000	-0.00751098	-0.00751098	-0.00683456	-0.00683456	
MEME J2000 (mean motion, ea, tau, kepl_period):						
-0.000000021	0.00000030	-0.00001116	0.00000040			
MEME J2000 (a,ag,af,chi,psi,mean long):						
-0.00000040	0.000000000	0.000000000	0.000000000	0.000000000	-0.00000004	
LLR - J2000 (dec,ra,r):						
0.000000334	0.000000368	-0.00071				
Mixed Spherical, MEME - J2000 (geodetic lat,lon,alt,hfpa,az,v):						
0.000000341	-0.000000064	-0.000203766	0.000000214	0.000000039	0.000000301	
Spherical, MEME-J2000 (ra,dec,rad,hfpa,azimuth,velocity):						
0.000000368	0.000000334	-0.000708099	0.000000214	0.000000039	0.000000301	
LLA, ECF (geodetic lat,lon,alt):						
0.000000341	-0.000000064	-0.000203766				
LLR, ECF (lat,lon,r):						

0.000000027 -0.000000064 -0.000708099

Table 20. Case v5

Test v5: Parameter differences in the sense Aerospace - STK
 GEO, Epoch at 1 Dec 2000, 18:23:58.410000
 Difference are in units of meters, meters/second, and degrees.

TETE of Date (x,y,z,xd,yd,zd):	-0.00875200	0.12091210	0.05370993	-0.00000848	0.00000017	0.00000081
TETE of Epoch (x,y,z,xd,yd,zd):	-0.00875200	0.12091210	0.05370993	-0.00000848	0.00000017	0.00000081
TEME of Date (x,y,z,xd,yd,zd):	-0.00705900	0.08823090	0.05051773	-0.00000574	-0.00000059	0.00000092
ECF (x,y,z,xd,yd,zd):	-0.01031400	0.03372800	0.05367039	0.00000062	-0.00000142	0.00553849
MEME - B1950 (x,y,z,xd,yd,zd):	-0.52480800	7.19962840	-17.43529750	-0.00052311	-0.00003198	0.00031270
(r,v):	0.00062826	-0.00000009				
MEME - J2000 (x,y,z,xd,yd,zd):	0.00000000	0.00000000	0.00000000	0.00000000	0.00000000	0.00000000
MEME J2000 (a,e,i,raan,arg_perigee,ta):	-0.00846601	-0.00000035	0.00000000	0.00000593	-0.00001843	0.00001153
MEME J2000 (ma,arg_lat,apogee_ht,apogee_per_ht,perigee):	0.00001224	-0.00000589	-0.03366017	-0.03366017	-0.05469147	-0.05469146
MEME J2000 (mean motion, ea, tau, kepl_period):	0.0000000005	0.00001207	0.00282995	-0.00002600		
MEME J2000 (a,ag,af,chi,psi,mean long):	-0.00846601	0.000000000	0.000000001	0.000000000	0.000000000	0.00000002
LLR - J2000 (dec,ra,r):	-0.000000222	0.000000035	0.00030			
Mixed Spherical, MEME - J2000 (geodetic lat,lon,alt,hfpa,az,v):	0.000000001	-0.000000141	0.000336707	-0.000000164	-0.000000105	-0.000000657
Spherical, MEME-J2000 (ra,dec,rad,hfpa,azimuth,velocity):	0.000000035	-0.000000222	0.000295997	-0.000000164	-0.000000105	-0.000000657
LLA, ECF (geodetic lat,lon,alt):	0.000000001	-0.000000141	0.000336707			
LLR, ECF (lat,lon,r):	0.000000285	-0.000000141	0.000295997			

Table 21. Case v6

Test v6: Parameter differences in the sense Aerospace - STK
 SEO, Epoch at 25 Dec 2010, 9:51:42.900000
 Difference are in units of meters, meters/second, and degrees.

TETE of Date (x,y,z,xd,yd,zd):						
-0.02052800	0.03024100	0.01896960	-0.00000202	-0.00000165	-0.00000049	
TETE of Epoch (x,y,z,xd,yd,zd):						
-0.02052800	0.03024100	0.01896960	-0.00000202	-0.00000165	-0.00000049	
TEME of Date (x,y,z,xd,yd,zd):						
-0.02804100	0.04218800	0.02549090	-0.00000356	-0.00000248	-0.00000048	
ECF (x,y,z,xd,yd,zd):						
-0.06210100	-0.11852000	0.01913570	-0.00026382	0.00000404	0.00529502	
MEME - B1950 (x,y,z,xd,yd,zd):						
7.76828200	-10.11768300	16.69440340	0.00046911	0.00050447	-0.00107451	
(r,v):						
0.00015197	-0.00000026					
MEME - J2000 (x,y,z,xd,yd,zd):						
0.00000000	0.00000000	0.00000000	0.00000000	0.00000000	0.00000000	
MEME J2000 (a,e,i,raan,arg_perigee,ta):						
-0.00000501	-0.00000008	-0.00000012	-0.00000025	-0.00000014	0.00000035	
MEME J2000 (ma,arg_lat,apogee_ht,apogee,per_ht,perigee):						
0.00000031	0.00000021	-0.03606915	-0.03606915	-0.03614444	-0.03614444	
MEME J2000 (mean motion, ea, tau, kepl_period):						
-0.0000000008	-0.00000010	0.00000013	-0.00000026			
MEME J2000 (a,ag,af,chi,psi,mean long):						
-0.00000501	0.00000000	0.00000000	0.00000000	0.00000000	0.00000000	
LLR - J2000 (dec,ra,r):						
-0.000000195	-0.000000179	0.00049				
Mixed Spherical, MEME - J2000 (geodetic lat,lon,alt,hfpa,az,v):						
0.000000457	-0.000000041	0.000312343	-0.000000408	0.000000314	-0.000000389	
Spherical, MEME-J2000 (ra,dec,rad,hfpa,azimuth,velocity):						
-0.000000179	-0.000000195	0.000491999	-0.000000408	0.000000314	-0.000000389	
LLA, ECF (geodetic lat,lon,alt):						
0.000000457	-0.000000041	0.000312343				
LLR, ECF (lat,lon,r):						
-0.000000063	-0.000000041	0.000491999				

2.5 Summary

The most frequently used orbital parameter set and coordinate frame transformations of the Satellite Tool Kit have been thoroughly exercised by the suite of validation procedures described in this report. Most of the differences between STK and the astrodynamic tools used at The Aerospace Corporation are due to the following causes:

- The number of significant digits output by a computer program.
- Implementation differences such as the determination of perigee and apogee passage.
- Algorithm difference such as the completely different approaches for the transformation of a vector from the ECF to the B1950/FK4 ECI MEME frame.

In general, there is agreement between the astrodynamic tools used at The Aerospace Corporation (TRACE v2.4.9, Rotate v1.0, and Geo v1.0) and STK v4.1.0. In the areas of parameter and coordinate frame transformations the validation results identify STK as a tool for precision astrodynamic analyses at the decimeter level. Precision is established at a level of less than 12 centimeters for position and six millimeters per second for velocity transformations from inertial reference frames to an Earth-centered and fixed reference frame.

3. Validation of STK Access and Visibility Functions

This section describes the IV&V of access and visibility calculations of the STK v4.1.0 software; the IV&V consisted of comparisons of output from STK with Aerospace-developed codes, and additional analyses were completed to resolve the source of any differences. The objective was to compare access and visibility data over a sufficiently broad range of vehicle, sensor, and target geometry such that confidence in the results of the IV&V would be high. Furthermore, the task was structured such that the individual cases reflected “typical” orbits, sensor constraints, and target locations likely to be of interest to a majority of AGI’s customer base while maintaining as many common elements as possible within the scenario designs. Consequently, the number of individual cases was quite large.

3.1 Validation Approach

The philosophy used in creating appropriate test cases was to design the validation program such that the software would be used in a manner similar to a majority of AGI’s customers, but to simplify the conditions wherever possible without altering, fundamentally at least, the numerical calculations being tested. Consequently, a WGS-84 reference ellipsoid was used in all scenarios, and a Keplerian propagator *without* J_2 effects was used to generate the ephemerides for all vehicles. A J_2 propagator is not substantially more complex than a two-body propagator, and access and visibility calculations are dependent only upon position and attitude of the satellite relative to the target. Consequently, using the simpler propagator has no negative impact to the results of the validation program. Satellite ephemerides could have been imported into STK thus guaranteeing that the vehicle positions were identical between the tools, but it was felt that there were substantial reasons to avoid this method. Foremost among these was to use the product in the same manner that the majority of AGI’s customers will use STK (i.e., creating vehicles and propagating them within the program). Secondary reasons for using internal propagation included the possibility that handling large data sets might increase the potential for errors, the loss of precision due to truncation and round-off, and the added value to the contract of “verifying” another propagator in addition to the work being completed under another task within the IV&V effort. Finally, we randomly checked STK satellite ephemerides against Aerospace tools for several cases and found the data to match within a few millimeters.

3.2 Tool Descriptions and Comparisons

The principal Aerospace software used in calculating the Aerospace data for the IV&V is a library of routines called ASTROLIB. The Aerospace Corporation has developed a number of other tools that include high-precision propagators and a visualization program similar to STK. However, the philosophy within the company has been to use an appropriate tool with appropriate modeling assumptions for the work to be performed. For example, most long-term access and visibility studies use ASTROLIB (1999 version) as the core program including, at most, secular J_2 effects, although they could reference stored ephemerides of higher propagated fidelity. Experience has shown that, in most cases, the differences in visibility statistics between using ASTROLIB and a higher-fidelity model are insignificant; even using a spherical Earth model instead of an ellipsoid frequently yields no significant differences in the visibility statistics. Since geoidal separation, local terrain, and masking due to buildings or trees can have greater influences on visibility than Earth orientation perturbations, and those terms are neglected because of the difficulty in modeling them, our approach has been to neglect all terms of the same order.

Analytical Graphics, on the other hand, has included the effects of nutation, precession, and pole-wander in all calculations regardless of the type of propagator or integrator being used. Their approach is that the

perturbations are well known, easily modeled, and therefore, can be included in even the simplest of propagators.

Beyond such basic underlying modeling differences, Aerospace programs operate differently than STK. For example, STK calculates the ephemerides of the vehicles and then interpolates between propagation time steps to determine the endpoints of an access interval whereas ASTROLIB iterates to an “exact” solution. If an STK user does not specify a sufficiently small time step, however, the accuracy of the results may suffer. With the approach used in ASTROLIB, results are independent of a user defined propagation time step, but the calculations require more time to complete. One approach is not necessarily better than the other, but one must keep in mind that all engineering tools include assumptions, approximations, and methodologies that can occasionally produce significantly different results from small modeling differences.

3.3 Scenario Design

3.3.1 Orbits

Three orbit regimes were chosen for the validation effort such that they reflect the most common types in use today: (1) a low Earth orbit (LEO), (2) a highly elliptical orbit (HEO), and (3) a geosynchronous orbit (GEO). Appropriate parameters were chosen for each orbit class and are shown in Table 22. We decided to use four different inclinations for the LEO orbits to examine access for a variety of passage geometry with respect to the ground target. An inclination of 35° for the GEO case was chosen to force target line-of-sight interruptions for some of the sensor patterns. In all cases the epoch for the orbits is 4/1/2000 00:00:00 UTC.

Table 22. Keplerian Orbital Elements for Scenarios

Class/Type	a (km)	e	i (deg)	Ω (deg)	ω (deg)	M (deg)
LEO	7378.137	0.0	0.0	270.0	0.0	0.0
	7378.137	0.0	30.0	270.0	0.0	0.0
	7378.137	0.0	60.0	270.0	0.0	0.0
	7378.137	0.0	90.0	270.0	0.0	0.0
HEO	26600.0	0.75	63.435	210.0	270.0	0.0
GEO	42164.17	0.0	35.0	186.793	0.0	0.0

3.3.2 Sensors

As with the orbit design, a similar philosophy was used when specifying the sensors. We wanted sensor footprints that were common and contained enough constraints to provide a thorough test of the software. Ultimately, nine sensor designs were chosen: (1) nadir – horizon, (2) in-track – horizon, (3) cross-track – horizon, (4) nadir – 10° elevation, (5) in-track – 10° elevation, (6) cross-track – 10° elevation, (7) forward-looking, (8) push-broom, and (9) side-looking. Figures 1 through 6 illustrate each of these sensors (except the 10° elevation constraints) through field-of-view (FOV) volumes from STK.

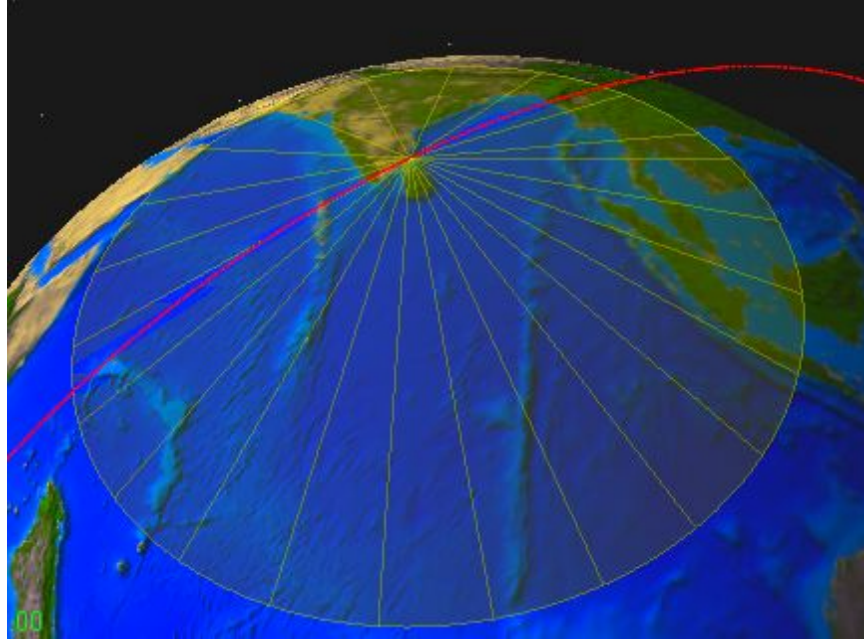


Figure 1. Nadir – horizon sensor

The sensor bore-sight is pointed along the spacecraft z-axis; there are no other FOV constraints.

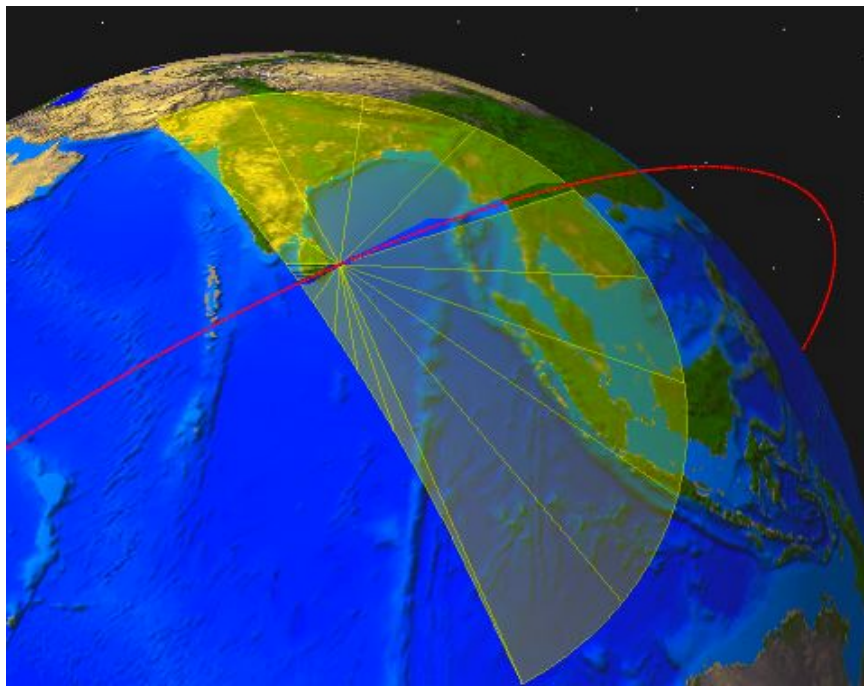


Figure 2. In-track – horizon sensor

The sensor bore-sight is pointed along the spacecraft z-axis; the FOV is constrained to azimuth angles between 270° and 90°.

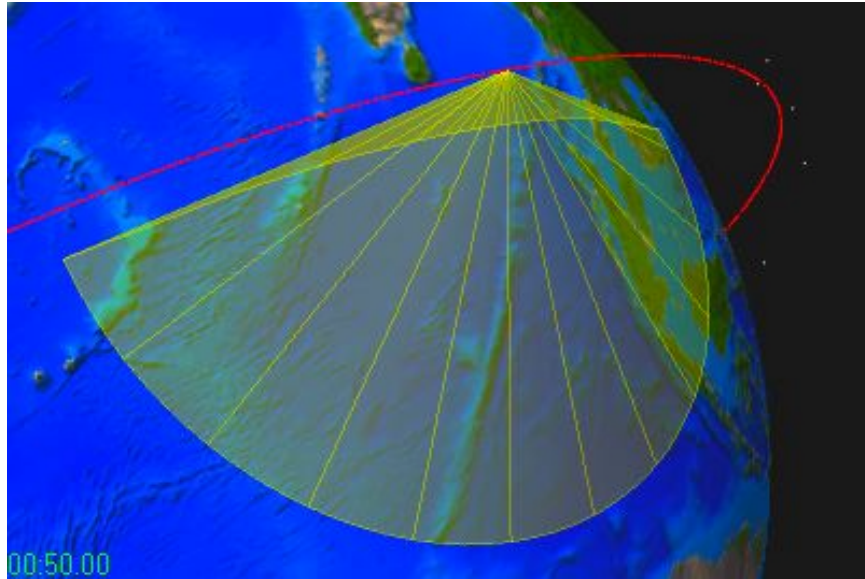


Figure 3. Cross-track – horizon sensor

The sensor bore-sight is pointed along the spacecraft z-axis; the FOV is constrained to azimuth angles between 0° and 180° .

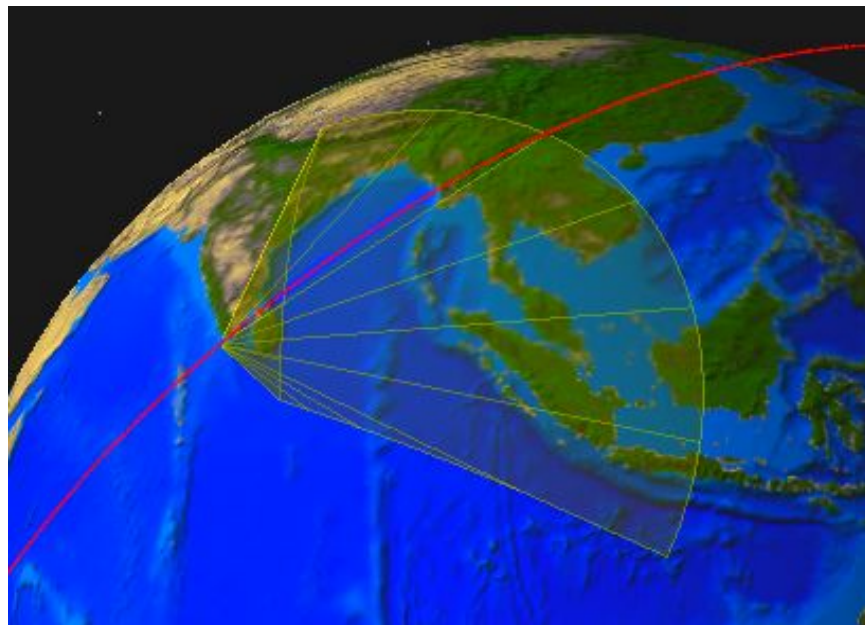


Figure 4. Forward-looking sensor

The sensor bore-sight is pointed along the spacecraft z-axis; the FOV is constrained to azimuth angles between 300° and 60° .

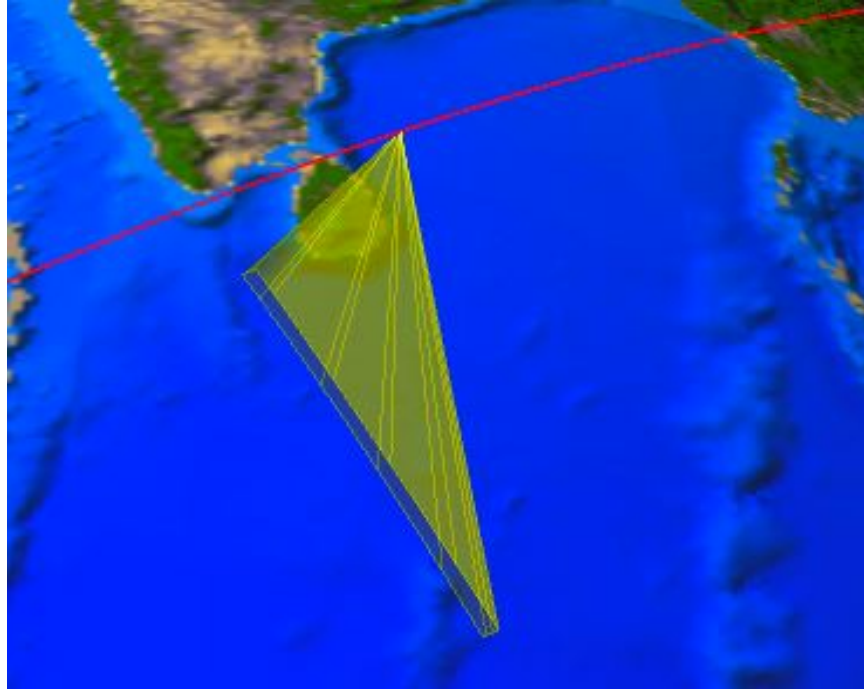


Figure 5. Push-broom sensor

The sensor bore-sight is pointed along the spacecraft velocity vector; the FOV is constrained to azimuth angles between 150° and 210° with minimum and maximum cone angles of 88° and 90° respectively.

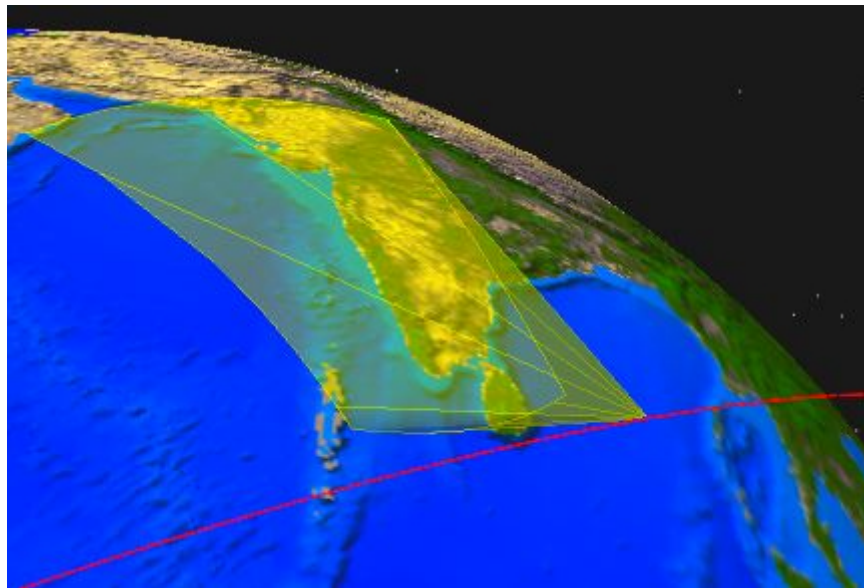


Figure 6. Side-looking sensor

The sensor bore-sight is pointed along the spacecraft cross-track direction; the FOV is constrained to azimuth angles between 150° and 270° and the maximum cone angle is 60° for LEO, 70° for HEO, and 85° for GEO vehicles.

3.3.3 Targets

Two primary ground targets were defined for the access calculations – 0° latitude, 0° longitude and 30° N latitude, 0° longitude. The 30° N, 0° E ground target was replaced with 30° N, 90° E for the GEO cases to test accesses near the edge of some of the sensor footprint patterns. A 10° by 10° box centered about 30° N, 0° E was defined by for access calculations to area targets. Users of STK should be aware that the number of points used to define the area target will make a difference in the access calculations. When we defined the area target with four points vs. populating the enclosed region with 121 points, the minimum access times varied by as much as a 1%. Consequently, we used the area target with 121 points in the course of this validation.

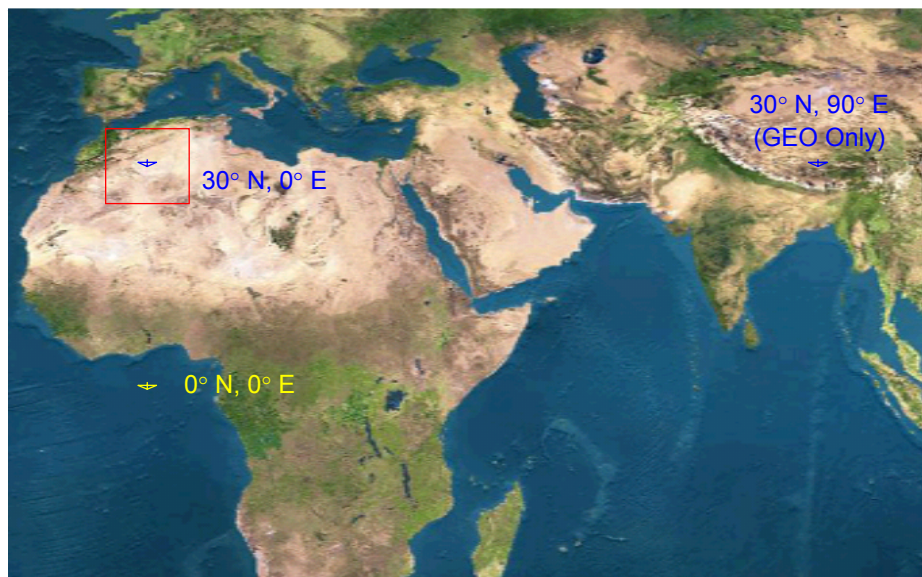


Figure 7. Point and Area Target Locations

3.3.4 Individual Satellite Visibility Case Naming Convention

We developed a naming convention for the test cases due to the large number involved. For example, if we were interested in the results for the 60° inclination LEO orbit, area target, and push-broom sensor, the case would appear in the results as *leo60_a_8*. The format and individual elements used in the naming convention are

			<i>orbit_target_sensor</i>
<i>orbit:</i>	geo	=	geosynchronous equatorial orbit
	heo	=	highly elliptical orbit
	leo0	=	low Earth orbit, 0° inclination
	leo30	=	low Earth orbit, 30° inclination
	leo60	=	low Earth orbit, 60° inclination
	leo90	=	low Earth orbit, 90° inclination
<i>target:</i>	0	=	0° latitude, 0° longitude
	30	=	30° N latitude, 0° longitude (90° E longitude for GEO)
	a	=	10° × 10° area target around 30° N latitude, 0° longitude

<i>sensor:</i>	1	=	nadir – horizon
	2	=	in-track – horizon
	3	=	cross-track – horizon
	4	=	nadir – 10° elevation
	5	=	in-track – 10° elevation
	6	=	cross-track – 10° elevation
	7	=	forward-looking
	8	=	push-broom
	9	=	side-looking

3.3.5 Satellite-to-Satellite Visibility Case Naming Convention

While validation of the access calculations for satellite to ground targets was the centerpiece of the study, we felt that an examination of satellite-to-satellite visibility was also needed. We chose three different cases that combine the orbit types discussed earlier and would be similar to practical applications. The CHAINS module of STK was used to construct the “flow” from the ground target, through the satellites, and finally to a ground station. The first satellite acted as the coverage element and was targeted, via a tracking sensor, on a desired ground location (30° N, 90° E or 0° N, 90° E). This satellite was then linked to a second satellite, which in turn was linked to a ground station located at 30° N, 0° E. Table 23 lists the elements of the cases chosen (orbital parameters for the spacecraft may be found in Table 22), and Figure 8 illustrates the locations of the ground targets and station. All of the cases listed were run with and without a satellite-to-satellite range constraint as shown in the table.

Table 23. Elements of the Satellite-to-Satellite Cases

Case	Coverage	Relay	Range (km)
leoheo	60° incl. LEO	HEO	45,000
leogeo	60° incl. LEO	GEO	45,000
heogeo	HEO	GEO	35,000

Ground Station: 30° N, 0° E with 5° elevation constraint
 Ground Targets: 0° N, 90° E and 30° N, 90° E



Figure 8. Ground Station and Point Target Locations

Case names for the satellite-to-satellite scenarios, shown below, are similar to the scenarios for individual satellites.

	<i>CoverageRelay_target_constraint</i>		
<i>coverage:</i>	heo	=	highly elliptical orbit
	leo	=	low Earth orbit, 60° inclination
<i>relay:</i>	geo	=	geosynchronous equatorial orbit
	heo	=	highly elliptical orbit
<i>target:</i>	0	=	0° latitude, 90° longitude
	30	=	30°N latitude, 90° longitude
<i>constraint:</i>	r	=	range limited
			LEO – 45,000 km
			HEO – 35,000 km

3.4 Results

There were four basic metrics that were used during the study for comparison between Satellite Tool Kit and The Aerospace Corporation software: (1) number of access intervals, (2) minimum access interval duration, (3) maximum access interval duration, and (4) cumulative access duration. While only a few of the cases will be presented here, a complete listing of results may be found in the Appendix.

Comparisons of the metrics concentrated on the differences in the STK results relative to those determined from the Aerospace tool set. Very simply, the relative error equation had the following form

$$\frac{(metric_{STK} - metric_{Aerospace})}{metric_{Aerospace}} \times 100\%$$

We decided that a relative error magnitude greater than 1% was sufficient to raise concerns about any particular case. From a total case count of 174, 20 cases had error percentages outside the prescribed bounds for at least one of the metrics. Most of the discrepancies between the tools were in the minimum access intervals which, of course, is the metric most sensitive to small differences.

3.4.1 Points and Areas

Samples of the results, including point and area targets, are presented in Tables 24 and 25. There is excellent agreement between the results from STK and Aerospace for a majority of the cases and metrics, frequently two orders of magnitude below the 1% threshold.

Table 24. Point Target Relative Differences for Selected Cases

Case	#	Min	Max	Ave	Total
leo30_30_8	0.00%	0.00%	0.00%	0.00%	0.00%
leo60_30_7	0.00%	2.12%	0.00%	0.00%	0.00%
heo_0_3	0.00%	0.00%	0.00%	0.00%	0.00%
heo_30_8	0.00%	-0.01%	-0.01%	0.00%	0.00%
geo_0_6	0.00%	-0.01%	0.00%	0.00%	0.00%
geo_0_9	0.00%	0.01%	0.01%	0.01%	0.01%

Table 25. Area Target Relative Differences for Selected Cases

Case	#	Min	Max	Ave	Total
leo30_a_1	0.00%	0.00%	0.00%	0.00%	0.00%
leo90_a_2	0.00%	-1.16%	0.00%	-0.04%	-0.04%
heo_a_4	0.00%	0.00%	0.00%	0.00%	0.00%
heo_a_7	0.00%	-0.59%	-0.02%	-0.13%	-0.13%
geo_a_2	0.00%	0.00%	0.00%	0.00%	0.00%
geo_a_6	0.00%	0.00%	0.00%	0.00%	0.00%

3.4.2 Satellite-to-Satellite

Of the 12 cases examined for the satellite-to-satellite study, all of the metrics (except the minimum access duration in two cases) were nearly identical; relative errors were also typically two orders of magnitude below the 1% threshold. Both cases that showed above threshold differences involved a LEO satellite relaying to a GEO vehicle, and the differences were only 2.1 seconds for one particular access. Errors of this magnitude are insignificant, particularly since the time units are in seconds, and have been shown to be directly related to the differences in modeling assumptions.

3.5 Data Verification Tests

After generating the data for all of the cases and creating tables for comparison, we began a series of tests to confirm that no errors had been made in the setup of the scenarios or handling of the data. In the first test, we used additional Aerospace tools to check the Aerospace data. When generating the STK data, we had divided the scenarios equally among the two engineers involved in the task; for the second test, we checked each other's work by using an independent scenario to duplicate the cases. In the third test, we used completely independent calculations of the geometry to determine the access times, but we used this technique for only a few representative cases because it is a rather lengthy process.

The independent calculations used in the third test varied depending upon the particular case. When the geometry was simple enough, a handheld calculator or spreadsheet was sufficient to check the data. For cases in which the geometry was more complex, the access times were created from the azimuth and elevation data by calculating the geometrical constraints of the sensor, the states of the vehicles, and applying the appropriate reference frame transformations. Clearly, this process was extremely time-consuming, but quite definitive in resolving differences in the results.

3.5.1 Resolution of the Differences

In 17 of the 174 cases included in the validation, STK v4.1.0 results showed differences in only the minimum access duration, and in only 3 cases, were there differences in more than one metric. We examined a few of these cases to verify that the source of the differences was due to the modeling issues addressed in the tool descriptions. Using the reporting features available in STK and ASTROLIB, we were able to quickly verify that the Earth-Centered Fixed (ECF) position of the targets and ECI positions

of the vehicles were identical within the expected numerical precision. Reports were also created to display the Greenwich Hour Angle from each tool, and the rotation, nutation, and precession matrices from STK. Using this data, we were then able to transform the Aerospace data to the same reference frames used in STK and match the ECI positions of the target. Similarly, we could reverse the transformation and show that the STK positions matched the ASTROLIB positions using the latter's frame of reference. Once the positions could be matched, it was a simple exercise to show that the sensor field-of-view constraints applied to the modified data produced results that were well within the 1% threshold.

The 3 cases for which more than one metric did not match require additional explanation. Two of these cases involve a LEO vehicle with an inclination of 0° accessing a target on the Equator with a sensor that excludes only the Northern Hemisphere of the ECI frame. This may appear to be a very strange combination, but the specifications of this case were designed to specifically highlight differences in Earth orientation parameters. Because the target moves in an inclined plane relative to the ECI frame in STK (due to the inclusion of perturbations), it is in the Northern Hemisphere for half the time; consequently, the number of accesses is substantially smaller. The Aerospace model, on the other hand, obtains an access on every pass because the target is always, at least within the machine precision, in the ECI equatorial plane.

The remaining case involved a LEO vehicle with an inclination of 90° accessing an area target with the forward-looking sensor. In this example, the Aerospace data includes an access that STK does not report. However, the graphics in the STK map window, as shown in Figure 9, indicates that there is an access to the area. When a single point target is placed at the corner of the area target shown in the figure (35° N, 5° W), the STK report indicates an access duration of 5.8 sec. This agrees reasonably well with the Aerospace result considering that access to the area would be slightly longer. This appears to be a minor problem, but we were unable to determine the cause, particularly when one considers that the area definition explicitly includes the corner points.

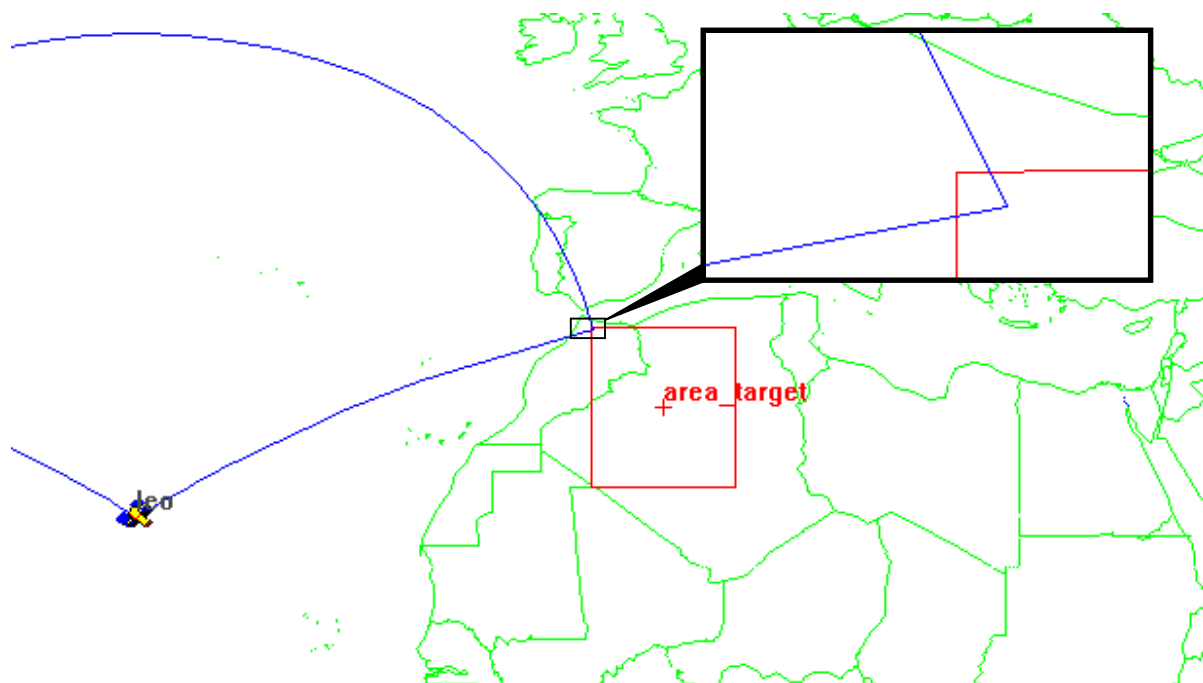


Figure 9. Forward-Looking Sensor Access to Area Target

3.6 Conclusions

The validation of the access and visibility computations in STK v4.1.0 was completed by comparing the data from 174 combinations of vehicles, sensors, and targets with results produced by similar programs developed by The Aerospace Corporation. The elements used in the scenarios were chosen to represent a broad spectrum of configurations, most of which are likely to be encountered by customers of AGI. It was found that 154 of the cases had nearly identical access and visibility statistics with differences usually within 0.01% or less. In 19 cases, the differences were a consequence of differences in modeling of the Earth orientation parameters. In particular, STK includes the effects of nutation, precession, and pole-wander whereas the Aerospace tool used in this validation program does not. The result is that the targets have slightly different inertial positions, by fractions of a kilometer, at any point in time. Under certain conditions, such as when an access occurs near the edge of a sensor cone, the duration may differ by several seconds, or in the worst case, may be missed altogether. For those 19 cases, we were able to compensate for the differences in modeling and show conclusively that the different results were entirely due the perturbations. For the one remaining case, the STK access report to the area target was not consistent with the graphical representation or the access report to point target co-located along the perimeter of the area. We were unable to determine the cause of the difference particularly since the area target definition included the same point. Although this minor problem will need to be addressed by AGI, it is important to note that the results for 173 of 174 cases (99.5%) matched extremely well, and we conclude that the access and visibility calculations in STK v4.1.0 are accurate and can be used with a high degree of confidence in the results.

Appendix: Access Results Raw Data for All Cases

Individual Satellite Visibility Case name = *orbit_target_sensor*

<i>orbit:</i>	geo	=	geosynchronous equatorial orbit
	heo	=	highly elliptical orbit
	leo0	=	low Earth orbit, 0° inclination
	leo30	=	low Earth orbit, 30° inclination
	leo60	=	low Earth orbit, 60° inclination
	leo90	=	low Earth orbit, 90° inclination
<i>target:</i>	0	=	0° latitude, 0° longitude
	30	=	30°N latitude, 0° longitude (90°E longitude for GEO)
	a	=	10° × 10° area target centered around 30°N latitude, 0° longitude
<i>sensor:</i>	1	=	nadir – horizon
	2	=	in-track – horizon
	3	=	cross-track – horizon
	4	=	nadir – 10° elevation
	5	=	in-track – 10° elevation
	6	=	cross-track – 10° elevation
	7	=	forward-looking
	8	=	push-broom
	9	=	side-looking

Satellite-to-Satellite Visibility Case name = *CoverageRelay_target_constraint*

<i>coverage:</i>	heo	=	highly elliptical orbit
	leo	=	low Earth orbit, 60° inclination
<i>relay:</i>	geo	=	geosynchronous equatorial orbit
	heo	=	highly elliptical orbit
<i>target:</i>	0	=	0° latitude, 90° longitude
	30	=	30°N latitude, 90° longitude
<i>constraint:</i>	r	=	range limited LEO – 45,000 km HEO – 35,000 km

Table A.1. STK v4.1.0 and Aerospace Tools Access Results for LEO Cases

Case name	Satellite Tool Kit Access Statistics (sec)					Aerospace Tools Access Statistics (sec)					STK Results Relative to Aerospace				
	#	Min	Max	Ave	Total	#	Min	Max	Ave	Total	#	Min	Max	Ave	Total
leo0_0_1	178	353.464	1140.954	1136.53	202302.323	178	353.43	1140.95	1136.53	202302.29	0.00%	0.01%	0.00%	0.00%	0.00%
leo0_0_2	178	353.464	570.477	569.258	101327.891	178	353.43	570.477	569.258	101327.86	0.00%	0.01%	0.00%	0.00%	0.00%
leo0_0_3	92	55.788	1140.954	1078.051	99180.713	178	353.43	570.477	569.258	101327.86	-48.31%	-84.22%	100.00%	89.38%	-2.12%
leo0_0_4	178	192.12	818.266	814.748	145025.114	178	192.086	818.266	814.748	145025.08	0.00%	0.02%	0.00%	0.00%	0.00%
leo0_0_5	178	192.12	409.133	407.914	72608.615	178	192.086	409.133	407.913	72608.58	0.00%	0.02%	0.00%	0.00%	0.00%
leo0_0_6	91	16.977	818.266	777.482	70750.858	178	192.086	409.133	407.913	72608.58	-48.88%	-91.16%	100.00%	90.60%	-2.56%
leo0_0_7	178	353.464	570.476	569.25	101326.434	178	353.43	570.477	569.258	101327.86	0.00%	0.01%	0.00%	0.00%	0.00%
leo0_0_8	177	5.931	5.931	5.931	1049.715	177	5.931	5.931	5.931	1049.72	0.00%	0.00%	0.00%	0.00%	0.00%
leo0_0_9	0	0	0	0	0	0	0	0	0	0	0.00%	0.00%	0.00%	0.00%	0.00%
leo0_30_1	177	157.017	157.727	157.372	27854.808	177	157.38	157.38	157.38	27856.32	0.00%	-0.23%	0.22%	-0.01%	-0.01%
leo0_30_2	177	78.508	78.863	78.686	13927.407	177	78.69	78.69	78.69	13928.16	0.00%	-0.23%	0.22%	-0.01%	-0.01%
leo0_30_3	0	0	0	0	0	0	0	0	0	0	0.00%	0.00%	0.00%	0.00%	0.00%
leo0_30_4	0	0	0	0	0	0	0	0	0	0	0.00%	0.00%	0.00%	0.00%	0.00%
leo0_30_5	0	0	0	0	0	0	0	0	0	0	0.00%	0.00%	0.00%	0.00%	0.00%
leo0_30_6	0	0	0	0	0	0	0	0	0	0	0.00%	0.00%	0.00%	0.00%	0.00%
leo0_30_7	0	0	0	0	0	0	0	0	0	0	0.00%	0.00%	0.00%	0.00%	0.00%
leo0_30_8	0	0	0	0	0	0	0	0	0	0	0.00%	0.00%	0.00%	0.00%	0.00%
leo0_30_9	177	157.017	157.727	157.372	27854.808	177	157.38	157.38	157.38	27856.32	0.00%	-0.23%	0.22%	-0.01%	-0.01%
leo30_0_1	177	153.893	1128.239	763.572	135152.28	177	153.791	1128.24	763.557	135149.57	0.00%	0.07%	0.00%	0.00%	0.00%
leo30_0_2	177	75.126	564.296	381.797	67577.995	177	75.075	564.296	381.789	67576.64	0.00%	0.07%	0.00%	0.00%	0.00%
leo30_0_3	94	153.893	1119.309	720.796	67754.86	94	153.791	1119.31	720.781	67753.42	0.00%	0.07%	0.00%	0.00%	0.00%
leo30_0_4	98	14.7	809.114	597.975	58601.563	98	14.515	809.114	597.965	58600.59	0.00%	1.27%	0.00%	0.00%	0.00%
leo30_0_5	98	14.7	404.733	299.347	29335.986	98	14.515	404.733	299.341	29335.41	0.00%	1.27%	0.00%	0.00%	0.00%
leo30_0_6	54	74.272	795.671	545.916	29479.454	54	74.213	795.67	545.91	29479.12	0.00%	0.08%	0.00%	0.00%	0.00%
leo30_0_7	122	15.953	563.898	315.756	38522.172	122	15.942	563.898	315.752	38521.77	0.00%	0.07%	0.00%	0.00%	0.00%
leo30_0_8	28	5.869	6.995	6.444	180.426	28	5.869	6.995	6.444	180.43	0.00%	0.00%	0.00%	0.00%	0.00%
leo30_0_9	75	156.513	406.689	291.034	21827.554	75	156.428	406.694	291.024	21826.79	0.00%	0.05%	0.00%	0.00%	0.00%
leo30_30_1	102	121.348	1132.044	952.468	97151.71	102	121.361	1132.04	952.471	97152.02	0.00%	-0.01%	0.00%	0.00%	0.00%
leo30_30_2	102	34.855	566.163	476.134	48565.626	102	34.862	566.163	476.135	48565.78	0.00%	-0.02%	0.00%	0.00%	0.00%
leo30_30_3	10	710.646	1132.044	986.207	9862.074	10	712.186	1132.04	987.121	9871.21	0.00%	-0.22%	0.00%	-0.09%	-0.09%
leo30_30_4	84	178.895	812.599	685.341	57568.658	84	178.912	812.599	685.345	57568.99	0.00%	-0.01%	0.00%	0.00%	0.00%
leo30_30_5	84	73.524	406.396	342.593	28777.82	84	73.533	406.396	342.595	28777.99	0.00%	-0.01%	0.00%	0.00%	0.00%
leo30_30_6	10	550.876	812.599	757.636	7576.355	10	552.416	812.599	758.178	7581.78	0.00%	-0.28%	0.00%	-0.07%	-0.07%
leo30_30_7	91	8.28	565.506	410.262	37333.81	91	8.282	565.504	410.264	37334.06	0.00%	-0.02%	0.00%	0.00%	0.00%
leo30_30_8	38	5.905	6.579	6.098	231.714	38	5.905	6.579	6.098	231.71	0.00%	0.00%	0.00%	0.00%	0.00%
leo30_30_9	64	121.348	369.524	261.867	16759.517	64	121.361	369.523	261.865	16759.38	0.00%	-0.01%	0.00%	0.00%	0.00%

Table A.1 (cont.). STK v4.1.0 and Aerospace Tools Access Results for LEO Cases

Case name	Satellite Tool Kit Access Statistics (sec)					Aerospace Tools Access Statistics (sec)					STK Results Relative to Aerospace				
	#	Min	Max	Ave	Total	#	Min	Max	Ave	Total	#	Min	Max	Ave	Total
leo60_0_1	67	101.535	1095.479	918.512	61540.289	67	101.04	1095.48	918.504	61539.76	0.00%	0.49%	0.00%	0.00%	0.00%
leo60_0_2	67	89	548.23	459.451	30783.204	67	88.754	548.23	459.448	30783.03	0.00%	0.28%	0.00%	0.00%	0.00%
leo60_0_3	39	101.535	1070.04	787.553	30714.569	39	101.04	1070.03	787.54	30714.07	0.00%	0.49%	0.00%	0.00%	0.00%
leo60_0_4	46	507.626	785.568	672.804	30948.971	46	507.67	785.567	672.804	30948.98	0.00%	-0.01%	0.00%	0.00%	0.00%
leo60_0_5	46	233.886	393.27	336.025	15457.162	46	233.909	393.271	336.027	15457.23	0.00%	-0.01%	0.00%	0.00%	0.00%
leo60_0_6	28	74.326	747.392	550.083	15402.313	28	74.622	747.379	550.083	15402.33	0.00%	-0.40%	0.00%	0.00%	0.00%
leo60_0_7	66	6.106	547.345	313.664	20701.855	66	6.145	547.358	313.667	20701.99	0.00%	-0.63%	0.00%	0.00%	0.00%
leo60_0_8	10	5.705	5.763	5.722	57.22	10	5.705	5.763	5.722	57.22	0.00%	0.00%	0.00%	0.00%	0.00%
leo60_0_9	28	205.562	349.146	269.655	7550.342	28	205.565	349.132	269.655	7550.34	0.00%	0.00%	0.00%	0.00%	0.00%
leo60_30_1	112	183.914	1099.453	791.489	88646.798	112	183.847	1099.45	791.48	88645.76	0.00%	0.04%	0.00%	0.00%	0.00%
leo60_30_2	112	89.555	552.209	395.609	44308.228	112	89.521	552.209	395.605	44307.77	0.00%	0.04%	0.00%	0.00%	0.00%
leo60_30_3	74	183.914	1085.308	722.474	53463.063	74	183.847	1085.3	722.463	53462.27	0.00%	0.04%	0.00%	0.00%	0.00%
leo60_30_4	65	28.618	789.019	624.416	40587.015	65	27.699	789.018	624.402	40586.15	0.00%	3.32%	0.00%	0.00%	0.00%
leo60_30_5	65	28.075	396.156	312.182	20291.799	65	27.616	396.157	312.176	20291.42	0.00%	1.66%	0.00%	0.00%	0.00%
leo60_30_6	37	28.618	788.442	609.36	22546.319	37	27.699	788.443	609.349	22545.9	0.00%	3.32%	0.00%	0.00%	0.00%
leo60_30_7	82	1.83	548.322	320.255	26260.888	82	1.792	548.33	320.251	26260.6	0.00%	2.12%	0.00%	0.00%	0.00%
leo60_30_8	9	5.741	6.704	5.868	52.812	9	5.741	6.705	5.868	52.81	0.00%	0.00%	-0.01%	0.00%	0.00%
leo60_30_9	37	38.092	387.113	262.729	9720.972	37	38.418	387.082	262.734	9721.14	0.00%	-0.85%	0.01%	0.00%	0.00%
leo90_0_1	66	447.235	1054.879	836.183	55188.072	66	447.38	1054.88	836.186	55188.25	0.00%	-0.03%	0.00%	0.00%	0.00%
leo90_0_2	66	186.048	528.029	417.597	27561.427	66	186.124	528.03	417.601	27561.69	0.00%	-0.04%	0.00%	0.00%	0.00%
leo90_0_3	38	220.795	1023.703	725.063	27552.388	38	221.228	1023.69	725.065	27552.46	0.00%	-0.20%	0.00%	0.00%	0.00%
leo90_0_4	46	389.824	756.441	612.183	28160.441	46	389.933	756.441	612.186	28160.57	0.00%	-0.03%	0.00%	0.00%	0.00%
leo90_0_5	46	170.481	378.802	305.626	14058.791	46	170.538	378.804	305.63	14058.97	0.00%	-0.03%	0.00%	0.00%	0.00%
leo90_0_6	28	71.45	710.095	502.739	14076.684	28	71.884	710.071	502.74	14076.73	0.00%	-0.60%	0.00%	0.00%	0.00%
leo90_0_7	56	2.514	527.003	314.671	17621.559	56	2.428	527.025	314.662	17621.07	0.00%	3.54%	0.00%	0.00%	0.00%
leo90_0_8	10	5.497	5.565	5.516	55.164	10	5.497	5.565	5.516	55.16	0.00%	0.00%	0.00%	0.00%	0.01%
leo90_0_9	28	200.558	371.166	278.5	7798.007	28	200.564	371.137	278.503	7798.08	0.00%	0.00%	0.01%	0.00%	0.00%
leo90_30_1	74	354.864	1058.606	857.164	63430.144	74	355.025	1058.61	857.166	63430.31	0.00%	-0.05%	0.00%	0.00%	0.00%
leo90_30_2	74	143.235	531.002	428.245	31690.137	74	143.318	531.004	428.248	31690.35	0.00%	-0.06%	0.00%	0.00%	0.00%
leo90_30_3	38	600.263	1057.481	883.702	33580.684	38	600.337	1057.48	883.728	33581.65	0.00%	-0.01%	0.00%	0.00%	0.00%
leo90_30_4	56	59.397	759.546	579.138	32431.731	56	60.126	759.544	579.154	32432.61	0.00%	-1.21%	0.00%	0.00%	0.00%
leo90_30_5	56	3.75	380.196	289.232	16196.981	56	4.116	380.199	289.241	16197.52	0.00%	-8.89%	0.00%	0.00%	0.00%
leo90_30_6	28	442.726	758.827	646.405	18099.328	28	442.796	758.83	646.436	18100.22	0.00%	-0.02%	0.00%	0.00%	0.00%
leo90_30_7	64	2.765	519.247	322.7	20652.777	64	2.822	519.232	322.7	20652.83	0.00%	-2.02%	0.00%	0.00%	0.00%
leo90_30_8	12	5.556	6.522	5.81	69.716	12	5.556	6.522	5.81	69.72	0.00%	0.00%	0.00%	0.00%	-0.01%
leo90_30_9	34	72.561	369.981	257.862	8767.3	34	72.176	370.033	257.857	8767.12	0.00%	0.53%	-0.01%	0.00%	0.00%

Table A.1 (cont.). STK v4.1.0 and Aerospace Tools Access Results for LEO Cases

Case name	Satellite Tool Kit Access Statistics (sec)					Aerospace Tools Access Statistics (sec)					STK Results Relative to Aerospace				
	#	Min	Max	Ave	Total	#	Min	Max	Ave	Total	#	Min	Max	Ave	Total
leo0_a_1	178	209.958	853.998	850.318	151356.52	178	209.921	853.937	850.319	151356.75	0.00%	0.02%	0.01%	0.00%	0.00%
leo0_a_2	178	209.958	521.518	519.735	92512.755	178	209.921	521.486	519.736	92512.92	0.00%	0.02%	0.01%	0.00%	0.00%
leo0_a_3	0	0	0	0	0	0	0	0	0	0	0.00%	0.00%	0.00%	0.00%	0.00%
leo0_a_4	0	0	0	0	0	0	0	0	0	0	0.00%	0.00%	0.00%	0.00%	0.00%
leo0_a_5	0	0	0	0	0	0	0	0	0	0	0.00%	0.00%	0.00%	0.00%	0.00%
leo0_a_6	0	0	0	0	0	0	0	0	0	0	0.00%	0.00%	0.00%	0.00%	0.00%
leo0_a_7	178	209.958	228.325	228.172	40614.583	178	209.921	228.277	228.174	40614.95	0.00%	0.02%	0.02%	0.00%	0.00%
leo0_a_8	0	0	0	0	0	0	0	0	0	0	0.00%	0.00%	0.00%	0.00%	0.00%
leo0_a_9	178	85.497	602.965	599.965	106793.706	178	85.918	605.93	603.009	107335.57	0.00%	-0.49%	-0.49%	-0.50%	-0.50%
leo30_a_1	112	428.362	1320.438	1133.682	126972.439	112	428.36	1320.44	1133.73	126977.29	0.00%	0.00%	0.00%	0.00%	0.00%
leo30_a_2	112	220.051	774.385	671.903	75253.144	112	220.047	774.387	673.115	75388.89	0.00%	0.00%	0.00%	-0.18%	-0.18%
leo30_a_3	46	247.652	1309.515	1148.39	52825.933	46	248.984	1310.39	1151.56	52971.51	0.00%	-0.53%	-0.07%	-0.27%	-0.27%
leo30_a_4	94	396.185	996.784	865.971	81401.283	94	396.189	996.807	866.068	81410.39	0.00%	0.00%	0.00%	-0.01%	-0.01%
leo30_a_5	94	214.958	613.883	534.69	50260.828	94	217.096	613.884	535.104	50299.78	0.00%	-0.98%	0.00%	-0.08%	-0.08%
leo30_a_6	46	87.702	989.743	857.708	39454.576	46	88.48	990.357	860.989	39605.47	0.00%	-0.88%	-0.06%	-0.38%	-0.38%
leo30_a_7	102	76.848	754.815	586.308	59803.402	102	76.887	754.817	586.515	59824.56	0.00%	-0.05%	0.00%	-0.04%	-0.04%
leo30_a_8	56	108.494	204.315	182.507	10220.37	56	108.328	204.274	182.323	10210.09	0.00%	0.15%	0.02%	0.10%	0.10%
leo30_a_9	102	178.612	650.756	455.026	46412.628	102	176.92	656.36	456.729	46586.34	0.00%	0.96%	-0.85%	-0.37%	-0.37%
leo60_a_1	122	141.317	1337.496	1054.836	128689.991	122	141.638	1337.5	1054.88	128695.71	0.00%	-0.23%	0.00%	0.00%	0.00%
leo60_a_2	122	39.779	791.396	639.287	77992.986	122	39.941	791.402	639.576	78028.3	0.00%	-0.41%	0.00%	-0.05%	-0.05%
leo60_a_3	84	396.611	1329.465	1061.658	89179.263	84	399.97	1329.46	1063.32	89319.17	0.00%	-0.84%	0.00%	-0.16%	-0.16%
leo60_a_4	91	66.991	1026.373	750.383	68284.882	91	67.465	1026.37	750.326	68279.64	0.00%	-0.70%	0.00%	0.01%	0.01%
leo60_a_5	91	6.138	635.006	477.585	43460.242	91	6.377	635.009	479.446	43629.57	0.00%	-3.75%	0.00%	-0.39%	-0.39%
leo60_a_6	66	229.307	1009.428	725.943	47912.213	66	230.394	1013.44	728.01	48048.66	0.00%	-0.47%	-0.40%	-0.28%	-0.28%
leo60_a_7	112	187.114	789.89	490.119	54893.368	112	195.874	789.899	490.309	54914.59	0.00%	-4.47%	0.00%	-0.04%	-0.04%
leo60_a_8	28	173.32	245.267	222.274	6223.668	28	172.104	245.265	221.581	6204.27	0.00%	0.71%	0.00%	0.31%	0.31%
leo60_a_9	54	54.512	597.167	426.556	23034.005	54	54.201	598.976	427.681	23094.8	0.00%	0.57%	-0.30%	-0.26%	-0.26%
leo90_a_1	94	240.968	1235.539	986.142	92697.386	94	241.19	1235.57	986.176	92700.59	0.00%	-0.09%	0.00%	0.00%	0.00%
leo90_a_2	94	92.613	718.54	590.422	55499.688	94	93.701	718.548	590.658	55521.88	0.00%	-1.16%	0.00%	-0.04%	-0.04%
leo90_a_3	55	96.409	1235.582	947.327	52102.997	55	96.893	1235.57	947.36	52104.79	0.00%	-0.50%	0.00%	0.00%	0.00%
leo90_a_4	68	62.198	936.492	773.011	52564.733	68	61.676	936.165	772.968	52561.79	0.00%	0.85%	0.03%	0.01%	0.01%
leo90_a_5	68	55.538	566.776	481.204	32721.887	68	55.283	566.778	481.869	32767.09	0.00%	0.46%	0.00%	-0.14%	-0.14%
leo90_a_6	44	13.489	936.167	692.031	30449.37	44	13.086	936.165	692.038	30449.68	0.00%	3.08%	0.00%	0.00%	0.00%
leo90_a_7	77	30.485	708.394	513.407	39532.356	78	8.653	708.272	507.258	39566.1	-1.28%	252.31%	0.02%	1.21%	-0.09%
leo90_a_8	24	182.364	184.598	183.545	4405.071	24	182.31	184.296	183.352	4400.44	0.00%	0.03%	0.16%	0.11%	0.11%
leo90_a_9	46	240.958	599.977	449.063	20656.9	46	241.19	600.244	449.268	20666.32	0.00%	-0.10%	-0.04%	-0.05%	-0.05%

Table A.2. STK v4.1.0 and Aerospace Tools Access Results for HEO Cases

Case name	Satellite Tool Kit Access Statistics (sec)					Aerospace Tools Access Statistics (sec)					STK Results Relative to Aerospace				
	#	Min	Max	Ave	Total	#	Min	Max	Ave	Total	#	Min	Max	Ave	Total
heo_0_1	15	43.378	41761.867	38948.485	584227.278	15	43.367	41761.9	38948.5	584227.44	0.00%	0.03%	0.00%	0.00%	0.00%
heo_0_2	29	43.378	16731.412	7657.709	222073.569	29	43.367	16732	7658	222082.1	0.00%	0.03%	0.00%	0.00%	0.00%
heo_0_3	14	37445.843	39964.131	38707.73	541908.227	14	37446.2	39964.5	38708.1	541913.21	0.00%	0.00%	0.00%	0.00%	0.00%
heo_0_4	14	41432.802	41543.639	41494.969	580929.563	14	41432.8	41543.7	41495	580929.81	0.00%	0.00%	0.00%	0.00%	0.00%
heo_0_5	28	608.715	16731.462	7878.993	220611.792	28	608.75	16732	7879.28	220619.77	0.00%	-0.01%	0.00%	0.00%	0.00%
heo_0_6	14	37299.357	39845.688	38576.633	540072.857	14	37299.7	39846.1	38577	540077.91	0.00%	0.00%	0.00%	0.00%	0.00%
heo_0_7	28	43.378	7768.932	2663.233	74570.521	28	43.367	7769.77	2663.97	74591.25	0.00%	0.03%	-0.01%	-0.03%	-0.03%
heo_0_8	42	44.749	3975.042	1380.524	57982.005	42	44.751	3975.07	1380.53	57982.06	0.00%	0.00%	0.00%	0.00%	0.00%
heo_0_9	5	44.869	320.083	198.279	991.397	5	44.565	319.983	198.117	990.59	0.00%	0.68%	0.03%	0.08%	0.08%
heo_30_1	14	40953.229	41043.931	41003.688	574051.631	14	40953.3	41043.9	41003.7	574051.87	0.00%	0.00%	0.00%	0.00%	0.00%
heo_30_2	28	1745.065	13235.596	6103.267	170891.468	28	1745.14	13236.7	6104	170912.01	0.00%	0.00%	-0.01%	-0.01%	-0.01%
heo_30_3	14	33132.109	35105.967	34313.739	480392.341	14	33132.3	35105.6	34313.8	480393.54	0.00%	0.00%	0.00%	0.00%	0.00%
heo_30_4	14	40603.164	40726.211	40671.761	569404.656	14	40603.2	40726.2	40671.8	569404.97	0.00%	0.00%	0.00%	0.00%	0.00%
heo_30_5	28	1575.63	13235.682	6022.511	168630.301	28	1575.71	13236.7	6023.2	168649.68	0.00%	0.00%	-0.01%	-0.01%	-0.01%
heo_30_6	14	32951.479	35105.967	34177.037	478478.524	14	32951.7	35105.6	34177.2	478480.3	0.00%	0.00%	0.00%	0.00%	0.00%
heo_30_7	15	878.472	1634.139	1181.463	17721.95	15	878.543	1641.29	1182.02	17730.36	0.00%	-0.01%	-0.44%	-0.05%	-0.05%
heo_30_8	32	253.274	11562.104	4212.737	134807.587	32	253.289	11563.4	4212.9	134812.74	0.00%	-0.01%	-0.01%	0.00%	0.00%
heo_30_9	7	2.281	461.423	255.993	1791.952	7	2.077	461.339	255.871	1791.1	0.00%	9.82%	0.02%	0.05%	0.05%
heo_a_1	28	8590.231	41220.379	25778.143	721788.013	28	8586.31	41220.5	25776.5	721743.24	0.00%	0.05%	0.00%	0.01%	0.01%
heo_a_2	42	2428.704	16384.821	8814.541	370210.713	42	2428.82	16385.8	8819.08	370401.38	0.00%	0.00%	-0.01%	-0.05%	-0.05%
heo_a_3	14	35223.759	37682.784	36463.104	510483.452	14	35224	37687.8	36465.1	510510.95	0.00%	0.00%	-0.01%	-0.01%	-0.01%
heo_a_4	14	40842.76	40929.618	40890.284	572463.972	14	40842.8	40929.9	40890.4	572466.11	0.00%	0.00%	0.00%	0.00%	0.00%
heo_a_5	28	2281.172	16384.817	8281.858	231892.028	28	2281.28	16385.8	8282.5	231909.85	0.00%	0.00%	-0.01%	-0.01%	-0.01%
heo_a_6	14	35064.277	37541.674	36312.207	508370.899	14	35064.5	37542.5	36314.3	508399.75	0.00%	0.00%	0.00%	-0.01%	-0.01%
heo_a_7	35	211.066	7983.252	2850.734	99775.678	35	212.328	7984.71	2854.42	99904.57	0.00%	-0.59%	-0.02%	-0.13%	-0.13%
heo_a_8	42	1244.367	16384.821	7195.089	302193.721	42	1244.43	16385.8	7200.31	302412.9	0.00%	-0.01%	-0.01%	-0.07%	-0.07%
heo_a_9	13	105.914	853.803	521.363	6777.718	13	105.855	853.742	521.324	6777.21	0.00%	0.06%	0.01%	0.01%	0.01%

Table A.3. STK v4.1.0 and Aerospace Tools Access Results for GEO Cases

Case name	Satellite Tool Kit Access Statistics (sec)					Aerospace Tools Access Statistics (sec)					STK Results Relative to Aerospace				
	#	Min	Max	Ave	Total	#	Min	Max	Ave	Total	#	Min	Max	Ave	Total
geo_0_1	1	1209600	1209600	1209600	1209600	1	1209600	1209600	1209600	1209600	0.00%	0.00%	0.00%	0.00%	0.00%
geo_0_2	29	3270.219	28767.712	27887.877	808748.422	29	3273.02	28773.5	27893.6	808913.74	0.00%	-0.09%	-0.02%	-0.02%	-0.02%
geo_0_3	15	3988.688	43082.037	40430.068	606451.018	15	3989.03	43082	40430.1	606451.31	0.00%	-0.01%	0.00%	0.00%	0.00%
geo_0_4	1	1209600	1209600	1209600	1209600	1	1209600	1209600	1209600	1209600	0.00%	0.00%	0.00%	0.00%	0.00%
geo_0_5	29	3270.219	28767.712	27887.877	808748.422	29	3273.02	28773.5	27893.6	808913.74	0.00%	-0.09%	-0.02%	-0.02%	-0.02%
geo_0_6	15	3988.688	43082.037	40430.068	606451.018	15	3989.03	43082	40430.1	606451.31	0.00%	-0.01%	0.00%	0.00%	0.00%
geo_0_7	29	655.711	5641.253	5468.951	158599.571	29	656.363	5644.69	5472.32	158697.32	0.00%	-0.10%	-0.06%	-0.06%	-0.06%
geo_0_8	29	3270.221	28767.71	27887.876	808748.405	29	3273.02	28773.5	27893.6	808913.74	0.00%	-0.09%	-0.02%	-0.02%	-0.02%
geo_0_9	14	13730.251	13730.342	13730.297	192224.163	14	13728.9	13728.9	13728.9	192204.4	0.00%	0.01%	0.01%	0.01%	0.01%
geo_30_1	1	1209600	1209600	1209600	1209600	1	1209600	1209600	1209600	1209600	0.00%	0.00%	0.00%	0.00%	0.00%
geo_30_2	1	1209600	1209600	1209600	1209600	1	1209600	1209600	1209600	1209600	0.00%	0.00%	0.00%	0.00%	0.00%
geo_30_3	15	402.484	16762.067	15671.38	235070.707	15	401.975	16760.4	15669.8	235046.95	0.00%	0.13%	0.01%	0.01%	0.01%
geo_30_4	15	19014.42	69695.994	65269.636	979044.543	15	19014.1	69695.4	65269.1	979036.82	0.00%	0.00%	0.00%	0.00%	0.00%
geo_30_5	15	19014.42	69695.994	65269.636	979044.543	15	19014.1	69695.4	65269.1	979036.82	0.00%	0.00%	0.00%	0.00%	0.00%
geo_30_6	15	402.484	16762.067	15671.38	235070.707	15	401.975	16760.4	15669.8	235046.95	0.00%	0.13%	0.01%	0.01%	0.01%
geo_30_7	15	28218.775	61142.853	57286.747	859301.199	15	28219.4	61144	57287.8	859317	0.00%	0.00%	0.00%	0.00%	0.00%
geo_30_8	14	8750.898	8751.586	8751.268	122517.749	14	8746.16	8746.73	8746.44	122450.21	0.00%	0.05%	0.06%	0.06%	0.06%
geo_30_9	14	36199.553	36199.573	36199.564	506793.894	14	36199.6	36199.6	36199.6	506794.82	0.00%	0.00%	0.00%	0.00%	0.00%
geo_a_1	1	1209600	1209600	1209600	1209600	1	1209600	1209600	1209600	1209600	0.00%	0.00%	0.00%	0.00%	0.00%
geo_a_2	15	29143.227	59770.889	56006.065	840090.976	15	29144.3	59773.8	56008.9	840132.93	0.00%	0.00%	0.00%	0.00%	0.00%
geo_a_3	14	25651.868	25651.932	25651.898	359126.569	14	25650.9	25650.9	25650.9	359113.17	0.00%	0.00%	0.00%	0.00%	0.00%
geo_a_4	1	1209600	1209600	1209600	1209600	1	1209600	1209600	1209600	1209600	0.00%	0.00%	0.00%	0.00%	0.00%
geo_a_5	15	29143.227	59770.889	56006.065	840090.976	15	29144.3	59773.8	56008.9	840132.93	0.00%	0.00%	0.00%	0.00%	0.00%
geo_a_6	14	25651.868	25651.932	25651.898	359126.569	14	25650.9	25650.9	25650.9	359113.17	0.00%	0.00%	0.00%	0.00%	0.00%
geo_a_7	15	13516.439	42727.322	40098.834	601482.513	15	13517.3	42728.6	40100.1	601501.25	0.00%	-0.01%	0.00%	0.00%	0.00%
geo_a_8	29	2163.918	32790.948	22792.08	660970.318	29	2162.41	32791.3	22792.3	660975.53	0.00%	0.07%	0.00%	0.00%	0.00%
geo_a_9	14	43123.792	43123.81	43123.797	603733.163	14	43124.1	43124.1	43124.1	603737.31	0.00%	0.00%	0.00%	0.00%	0.00%

Table A.4. STK v4.1.0 and Aerospace Tools Access Results for Satellite-to-Satellite Cases

Case name	Satellite Tool Kit Access Statistics (sec)					Aerospace tools Access Statistics (sec)					STK Results Relative to Aerospace				
	#	Min	Max	Ave	Total	#	Min	Max	Ave	Total	#	Min	Max	Ave	Total
leoheo_p1	33	127.174	1095.096	781.24	25780.934	33	127.52	1095.1	781.212	25780	0.00%	-0.27%	0.00%	0.00%	0.00%
leoheo_p1r	27	160.38	1095.096	805.784	21756.161	27	160.314	1095.1	805.709	21754.14	0.00%	0.04%	0.00%	0.01%	0.01%
leoheo_p2	86	167.451	1099.313	778.196	66924.827	86	167.416	1099.31	778.185	66923.92	0.00%	0.02%	0.00%	0.00%	0.00%
leoheo_p2r	50	22.217	1099.313	856.907	42845.344	50	22.317	1099.31	856.886	42844.28	0.00%	-0.45%	0.00%	0.00%	0.00%
heogeo_p1	8	4502.969	28973.352	16350.563	130804.503	8	4498.01	28964.6	16340.7	130725.78	0.00%	0.11%	0.03%	0.06%	0.06%
heogeo_p1r	8	4502.969	28973.352	16350.563	130804.503	8	4498.01	28964.6	16340.7	130725.78	0.00%	0.11%	0.03%	0.06%	0.06%
heogeo_p2	28	27235.747	38510.552	33568.422	939915.818	28	27236.6	38510.3	33568.6	939921.38	0.00%	0.00%	0.00%	0.00%	0.00%
heogeo_p2r	14	36885.664	38510.552	37753.995	528555.925	14	36885.3	38510.3	37753.7	528551.72	0.00%	0.00%	0.00%	0.00%	0.00%
leogeo_p1	75	15.67	1095.096	802.807	60210.521	75	17.997	1095.1	802.695	60202.15	0.00%	-12.93%	0.00%	0.01%	0.01%
leogeo_p1r	75	15.67	1095.096	760.913	57068.451	75	17.997	1095.1	760.926	57069.48	0.00%	-12.93%	0.00%	0.00%	0.00%
leogeo_p2	112	82.4	1099.313	754.795	84537.021	112	82.368	1099.31	754.327	84484.57	0.00%	0.04%	0.00%	0.06%	0.06%
leogeo_p2r	111	2.949	1099.313	744.61	82651.678	111	2.937	1099.31	744.593	82649.79	0.00%	0.41%	0.00%	0.00%	0.00%